Two quasi-particle excitations with particle-hole core polarization in even-even single closed shell nuclei

V. Gillet, B. Giraud, M. Rho

Classification
Physics Abstracts
4.161 — 4.165

TWO QUASI-PARTICLE EXCITATIONS WITH PARTICLE-HOLE CORE POLARIZATION IN EVEN-EVEN SINGLE CLOSED SHELL NUCLEI

V. GILLET, B. GIRAUD and M. RHO

Service de Physique Théorique, Centre d'Etudes Nucléaires de Saclay
BP n° 2, 91190 Gif-sur-Yvette, France

(*Reçu le 30 octobre 1975, accepté le 20 novembre 1975*)

Résumé. — Les énergies et les propriétés de transition des isotones pairs-pairs $N = 28$, 50 et des isotopes $Z = 28$, 50, 82 sont calculées dans le cadre de l'approximation des phases au hasard avec une interaction effective centrale dans un espace de configuration constitué par des composantes à 2 quasi-particules pour la couche ouverte et à 1 particule-1 trou pour le cœur fermé. A l'aide des résultats de la méthode d'inversion des équations du Gap, pratiquement toutes les données nécessaires (énergie de quasi-particule individuelle, intensité de la force) sont extraites des spectres des noyaux de masse impaire. Les rapports entre les différentes composantes de la force sont fixés à des valeurs constantes pour tous les noyaux étudiés et aucune charge effective n'est utilisée. Un accord d'ensemble excellent est obtenu pour les énergies des états vibrationnels. Par contre, en ce qui concerne les propriétés de transition, bien que celles des états 3^- soient toujours bien reproduites, celles des états 2^+ et 4^+ sont souvent trop petites d'un ordre de grandeur.

Abstract. — The energies and transition properties of the even-even $N = 28$, 50 isotones and $Z = 28$, 50, 82 isotopes are calculated in the framework of the Tamm-Dancoff and Random Phase Approximation, with an effective central interaction in an extended space consisting of two quasi-particle configurations for the open shell and particle-hole configurations for the closed core. Using the results of the Inverse Gap Equation Method, practically all the necessary input data (single quasi-particle energies, force strength) are extracted from the odd-mass nuclei. The ratios of the force components are kept to fixed values for all studied nuclei and no effective charge is used. An overall excellent agreement is obtained for the energies of the vibrational states. On the other hand, while the transition properties of the 3^- states are always well reproduced, those of the 2^+ and 4^+ states are often too small by about one order of magnitude.

1. **Introduction.** — We present here the results of an extensive program of calculation carried out for all even single-closed-shell (S.C.S.) nuclei, except the $N = 82$ isotones. We have calculated the vibrational state energies and transition properties in the isotones with $N = 28$, 50 and the isotopes with $Z = 28$, 50, 82. The general framework of the study is the spherical shell model, and the Tamm Dancoff or the Random Phase Approximations. The calculated spectrum of low-lying excitations is given by the diagonalization of an effective central finite range interaction in the space consisting of : i) two-quasi-particle configurations (arising from the open and closed neutron shells in the S.C.S. isotopes or the open and closed proton shells in the S.C.S. isotones) and ii) one-particle-one-hole configurations (arising from the other core particles). The present treatment differs from previous works [1] in many ways, in its conception as well as in the computational procedure (size of the configuration space, determination of the parameters, etc...). They can be summarized by the following points :

1) The study is extended to a large number of nuclei, throughout the mass table, so that an overall systematics of the results within the approximations used can be done, and their meaningfulness can be assessed within the uncertainties of any shell model calculation. In particular, the increase in collectivity brought by the Random Phase Approximation (R.P.A.) is discussed both for light and heavy nuclei and with or without the inclusion of core polarization limited to the particle-hole space.

2) The present approach to spectroscopic calculations involves almost no adjustable parameters such as Hartree-Fock energies and force strength. In a way it is a continuation of the phenomenological analysis of the odd-even single closed shell nuclear spectra carried out with the inverse gap equation (I.G.E.) method [2]. With this method practically all

the necessary input data for the present calculation can be extracted from the neighbouring odd mass nuclei. Specifically : *a*) the quasi-particle energies as well as core particle and hole energies are obtained from the states which are strongly excited in one nucleon transfer experiments, i.e. states which have large single particle spectroscopic factors, *b*) quasi-particle wave functions (the u's and v's of the B.C.S. state) and the effective strength V_0 of the $T = 1$, $S = 0$ central force are uniquely determined from experimental data by means of their analysis with the I.G.E. method [2]. The only adjustable parameter of the calculation, which has a meaningful effect on the results, is the $T = 0$, $S = 1$ strength. Its ratio to the V_0 strength has been kept fixed to the value 1.25 throughout the table. Likewise the less important odd state strengths $T = 1$, $S = 1$, $T = 0$, $S = 0$ have been kept fixed for all nuclei with the generally accepted values $-0.4\ V_0$ and V_0 respectively. The range of the gaussian force is 1.7 fermi and the harmonic oscillator parameters are given by electron scattering experiments. Hence, we are not looking for an agreement with all nuclei at the cost of using heavy parameter adjustments from region to region. Rather we wish to see whether one can get an over-all fair agreement of the position and transition properties of all vibrational states of S.C.S. nuclei. This approach, we hope, should make more apparent the agreements or disagreements obtained with the simple description usually utilized for these nuclei and which we adopt also here : B.C.S. approximation for the ground state, and mixing of two quasi-particle configurations in the open shell and particle-hole configurations for the core [1].

3) No effective charge is used in the calculation of transition probabilities. This allows a clear discussion of the effect of extending the configuration space from the usual two quasi-particle description to the core particle-hole excitations. More precisely two discussions are in order : i) the contribution of the core as compared to that of the open shells; ii) the validity of the particle-hole approximation for the core polarization. It is particularly interesting to compare systematically the results obtained for nuclei with open neutron shells (where the electromagnetic transition can occur only via core excitation) with nuclei with open proton shells (where both core and open shells contribute). We shall also compare systematically the calculated electromagnetic $B(E\lambda)$ with the corresponding $\Delta T = 0$ and $\Delta T = 1$ values. In the collective description of vibrational states, these various $B(E\lambda)$ are related to the same deformation parameter β_2, while in the microscopic description used here, they correspond to different parts of the nuclear wave function.

The many previous works on the subject [1] have shown that the overall picture used here is fairly consistent with the large amount of experimental data on vibrational states of S.C.S. nuclei. The motivation of the work such as it appeared from the above points is thus fourfold : 1) a unified calculation of all S.C.S. nuclei; 2) to link the I.G.E. phenomenological analysis of single particle states in odd-even nuclei with the properties of vibrational states in even-even nuclei; 3) the elimination of the effective force and effective charge parameter adjustments; 4) to furnish a complete set of wave functions for experimental tests.

The paper is organized in the following way. In section 2, we outline the theoretical ingredients as well as what is put in as inputs. This is followed by our results in section 3 : the first part deals with the general features, the second part with more detailed discussion of the results. Our points are illustrated by tables and figures. We also give the obtained wave functions so as to be readily accessible for further tests of the model.

Preliminary results have been given in two previous letters, references [3] and [4].

2. **Formalism and input data.** — The general formalism used is well known [5]. We shall differ from other treatments only in the way we determine the input parameters of the problem, and in some cases by the extended size of the configuration space. Thus, we shall recall only briefly the usual microscopic description of vibrations in single-closed-shell nuclei. This is intended for the specifications of phases and notations.

The ground state of a system with an open shell of identical nucleons is assumed to be fairly well represented by a pairing B.C.S. state for the valence nucleons and by closed shells for the core particles. However, it has been shown in a previous work [2] that pairing correlations lead to some breaking of shell closure. In order to bring in this effect, we shall distinguish between the particles which make up the open shell i.e. protons for isotones, neutrons for isotopes, and the other nucleons. The former will be described by the B.C.S. state, regardless of whether the particles belong to the open shell or to the core. This state has been calculated in reference. The other nucleons, i.e. neutrons for isotones, protons for isotopes, will be described by a single Slater determinant corresponding to shell closure. Thus, relatively to that reference ground state, denoted by $|\ \rangle$, we shall consider a configurational space made of two quasi-particle or particle-hole configurations :

$$|\ j_\alpha j_\beta\, JM\ \rangle = [\xi^+_\alpha\ \xi^+_\beta]^J_M = \frac{1}{\sqrt{1+\delta_{\alpha\beta}}} \times \sum_{m_\alpha m_\beta} (j_\alpha j_\beta\, m_\alpha\, m_\beta \mid JM)\ \xi^+_{j_\alpha m_\alpha}\ \xi^+_{j_\beta m_\alpha} |\ \rangle\,, \qquad (1)$$

where the creation operators ξ^+_{jm} for quasi-particles are defined in terms of the creation and annihilation operators η^+_{jm}, η_{jm} for nucleons by

$$\xi^+_{jm} = u_j\, \eta^+_{jm} + (-)^{j+m} v_j\, \eta_{j-m}\,. \qquad (2)$$

In the particle-hole limit, we have $u_\alpha = 1$, $v_\alpha = 0$ for the *particle* and $u_\beta = 0$, $v_\beta = 1$ for the *hole*.

The two-body force V is chosen here to be central with a Gaussian radial dependence of the form

$$V(r) = V_0 \, e^{-(r/\mu)^2} \times \\ \times \{ P_1^\tau \, P_0^\sigma + a P_0^\tau \, P_1^\sigma + b P_1^\tau \, P_1^\sigma + c P_0^\tau \, P_0^\sigma \}, \quad (3)$$

where we have introduced the projectors P_T^τ, P_S^σ in isospin and spin spaces on state T, S respectively. Hence with our definition V_0 is the strength of the $T = 1$, $S = 0$ part of the force. This strength, which is specific to the nuclear pairing effect, will be extracted from the inverse gap equation analysis as discussed below. The coefficients a, b, c, are the ratios of the other components of the force relative to the $T = 1$, $S = 0$ strength.

In the Random Phase Approximation (R.P.A.), correlations are allowed in the ground state and the excited states $\Psi_{JM}^{(i)}$ are assumed to differ from this ground state $| g \rangle$ by the presence or the absence of at most one quasi-particle pair

$$\Psi_{JM}^{(i)} = \sum_{\alpha\beta} \times \\ \times \{ X_{\alpha\beta}^{(i)} [\xi_\alpha^+ \, \xi_\beta^+]_M^J - (-)^{J+M} \, Y_{\alpha\beta}^{(i)} [\xi_\alpha \, \xi_\beta]_{-M}^J \} \, | g \rangle, \quad (4)$$

where the X and Y are solutions of the secular problem

$$\sum_{\alpha'\beta'} \{ ((E_\alpha + E_\beta) \, \delta_{\alpha\alpha'} \, \delta_{\beta\beta'} + \langle \alpha\beta \, | \, V \, | \, \alpha' \, \beta' \rangle) \times \\ \times X_{\alpha'\beta'}^{(i)} + \langle \alpha\beta \, | \, V \, | \, \widetilde{\alpha' \, \beta'} \rangle \, Y_{\alpha'\beta'}^{(i)} \} = E^{(i)} \, X_{\alpha\beta}^{(i)}$$

$$\sum_{\alpha'\beta'} \{ ((E_\alpha + E_\beta) \, \delta_{\alpha\alpha'} \, \delta_{\beta\beta'} + \langle \alpha\beta \, | \, V \, | \, \alpha' \, \beta' \rangle) \times \\ \times Y_{\alpha'\beta'}^{(i)} + \langle \alpha\beta \, | \, V \, | \, \widetilde{\alpha' \, \beta'} \rangle \, X_{\alpha'\beta'}^{(i)} \} = - E^{(i)} \, Y_{\alpha\beta}^{(i)}. \quad (5)$$

In these expressions the matrix elements between the two-quasi-particle configurations of eq. (1) and the corresponding time reversed state $| \widetilde{\alpha\beta} \rangle$ appear. The detailed expressions for the matrix elements are given in the appendix.

The transition probabilities from the ground state with spin 0 to the excited state of spin J thus calculated are expressed in terms of their $B(EJ)$ values usually defined as

$$B(EJ) = \sum_M \left| \sum_{\alpha\beta} (X_{\alpha\beta}^J + (-)^J \, Y_{\alpha\beta}^J) \times \right. \\ \left. \times \langle \alpha \, | \sum_{i=1}^N P(i) \, r_i^J \, Y_M^J(\hat{r}_i) \, | \, \beta \rangle \right|^2. \quad (6)$$

According to the case $P(i)$ is a projector on the proton coordinates for electromagnetic transitions, i.e. $P(i) = 1 - \tau_z(i)$, or a projector on the $\Delta t = 0$ part of the excitation, $P(i) = 1$ (which yields the relevant $B(EJ)$ for inelastic α-scattering), or finally a projector on the $\Delta T = 1$ part of the transition, $P(i) = +1$ for protons, -1 for neutrons. Proton inelastic scattering for example involves both the $\Delta T = 0$ and $\Delta T = 1$ amplitudes.

The Tamm-Dancoff limit consists in setting in all above expressions $Y = 0$. The detailed expression for the two-body and one-body matrix elements appearing in the above formula are given in the appendix in terms of the quasi-particle amplitudes u and v.

In the secular problems of eq. (5), the input parameters are the quasi-particle energies $E_\alpha + E_\beta$, the quasi-particle amplitudes u and v, and the force parameters. In analogy with calculations in doubly magic nuclei, the unperturbed quasi-particle, particle and hole energies are obtained from the spectra of odd even nuclei. The chosen states are those which are most strongly excited in single-particle transfer experiments with large single-particle spectroscopic factors. In fact we know from theory and experiment that such states may differ considerably from an independent particle description. Moreover the phenomenological analysis performed in the framework of the I.G.E. method has shown the limitation of the independent quasi-particle picture for the open shell odd-even nuclei. However, for doubly magic nuclei, although the neighbouring odd A nuclei deviate strongly from a pure shell model description, the use of their *dressed* experimental *single-particle* energies is a considerable factor in the success of usual particle-hole calculations. Similarly we shall utilise here the experimental values for the quasi-particle and particle-hole energies $E_\alpha + E_\beta$, and assume the corresponding wave functions to be approximated by the B.C.S. or shell model ones. In the case of quasi-particle states, the u and v's are determined uniquely from the experimental quasi-particle energies with the use of the I.G.E. procedure.

The experimental values for the E_ν and the corresponding extracted quantities V_0 and v_ν have been given for all the odd-even nuclei in a previous paper [2]. For the even-even nuclei the v's and V_0's are obtained by interpolating these values. Of course, the values obtained for V_0 depend on the size of the configuration space allowed for pairs. Thus in reference [2] two different values for V_0 were found for each nucleus according to whether only the open shell was taken into account or both the open shell and the nearest major shell were included. These two values are used here according to whichever of these two spaces is utilized. A direct test of the validity of the quasi-particle picture for odd-even S.C.S. nuclei is given by the variations of the parameter V_0 throughout each considered nuclear region. If the B.C.S. picture is fairly valid its variations should be small. Indeed the observed variations are generally less than one MeV [2]. The particle and hole energies for the closed shell, i.e. the protons in the case of the isotopes and the neutrons in the case of the isotones, are obtained from the spectra of the corresponding odd-even nuclei as observed in single particle transfer or pick up reactions.

The odd state components of the force, eq. (3), play a minor role in the results. We adopt the generally accepted value of -0.4 for the parameter b while c is totally undetermined because of its small statistical weight and we choose it equal to 1. The only significant adjustable parameter left is the triplet-even force $T = 0$, $S = 1$ which acts between protons and neutrons and which turn out to be important in the coupling of the core particles to the valence particles. Its ratio to the $T = 1$, $S = 0$ force, i.e. the parameter a of eq. (3) is chosen equal to 1.25 throughout the whole calculation (in most spectroscopic calculations it varies between 1.1 and 1.4). Since we are not attempting to make a precise fit of experiment, this value is to a certain extent arbitrary. However the important points we are driving at are not expected to depend on the precise value of this ratio.

The size of the configuration space is an important parameter of the problem. In order to study this effect, the calculation is done in three steps : First, only the open shell configurations are considered. Second, the configuration space is limited to the particle-hole excitations of the core alone (both protons and neutrons being treated on the same footing so as not to violate isospin conservation). Finally, all configurations in the open and closed shells are included. The single particle states which are included in these various cases are given in table I.

Before discussing the results, we wish to emphasize the very strong inherent limitations of such studies based on a phenomenological use of experimental single quasi-particle energies within a limited configuration space. Let us briefly recall here that the use of experimental energies already modifies deeply the meaning of the shell model matrix elements, apart from the force renormalisation due to the space truncation. This can easily be seen by considering the expansion of the true states $| \alpha \rangle$ of the odd A nuclei on some complete basis which we shall denote by $| i \rangle$,

$$| \alpha \rangle = \sum_i C_i^\alpha | i \rangle . \tag{7}$$

The use of the true eigenvalues $E_\alpha + E_\beta$ requires that we write the Schrödinger problem on the redundant basis made of states $| \alpha \rangle$,

$$\sum_{\alpha'\beta'} \left[(E_{\alpha'} + E_{\beta'}) \, \delta_{\alpha\alpha'} \, \delta_{\beta\beta'} + \right.$$
$$\left. + \sum_{ij i'j'} C_i^\alpha \, C_j^\beta \, C_{i'}^{\alpha'} \, C_{j'}^{\beta'} \, \langle ij \mid V \mid i'j' \rangle \right] X_{\alpha'\beta'} = E X_{\alpha\beta} . \tag{8}$$

However in practice the matrix elements are those constructed on single particle or single quasi-particle

TABLE I

Single-particle configurations designated in numerical order for use in tables VI *and* VII. *The corresponding experimental quasi-particle energies have been given in reference* [2]

	Two major shells												
	One major shell												
$N = 28$													
N	7	8	9	10	11			6	5	4			
nlj	$1f_{7/2}$	$2p_{3/2}$	$1f_{5/2}$	$2p_{1/2}$	$1g_{9/2}$			$1d_{3/2}$	$2s_{1/2}$	$1d_{5/2}$			
$Z = 28$													
N	8	9	10	11				4	5	6	7		
nlj	$2p_{3/2}$	$1f_{5/2}$	$2p_{1/2}$	$1g_{9/2}$				$1d_{5/2}$	$2s_{1/2}$	$1d_{3/2}$	$1f_{7/2}$		
$N = 50$													
N	11	10	9	8				12	13	14	15	16	
nlj	$1g_{9/2}$	$2p_{1/2}$	$1f_{5/2}$	$2p_{3/2}$				$1g_{7/2}$	$2d_{5/2}$	$2d_{3/2}$	$3s_{1/2}$	$1h_{11/2}$	
$Z = 50$													
N	12	13	14	15	16			11	10	9	8		
nlj	$1g_{7/2}$	$2d_{5/2}$	$2d_{3/2}$	$3s_{1/2}$	$1h_{11/2}$			$1g_{9/2}$	$2p_{1/2}$	$1f_{5/2}$	$2p_{3/2}$		
$Z = 82$													
N	23	22	21	19	20	18	17	24	25	26	27	28	29
nlj	$2g_{9/2}$	$1i_{13/2}$	$3p_{1/2}$	$2f_{5/2}$	$3p_{3/2}$	$2f_{7/2}$	$1h_{9/2}$	$3d_{5/2}$	$1i_{11/2}$	$2g_{7/2}$	$4s_{1/2}$	$3d_{3/2}$	$1j_{15/2}$

states. This assumes that the expansion (7) can be limited to only one term

$$| \alpha \rangle \approx C^{\alpha}_{i_0} | i_0 \rangle + \cdots \tag{9}$$

where $| i_0 \rangle$ is a shell model single particle or a B.C.S. single quasi-particle state. This is true only if the spectroscopic factors of the states $| \alpha \rangle$ identified as single particle or single quasi-particle states are large and close to 1. This is never the case and in fact, in the best of situations, they are only of the order of 0.8-0.9. In many cases they are even lower. Thus we see that each matrix element is weighted by a factor which can vary widely according to the various two-quasi-particle or particle-hole configurations which are considered. Such an effect cannot be absorbed by a renormalization of the force.

We wish to recall also the limitation introduced by the use of a limited configuration space. Let us consider the nuclear wave function given by the expansion

$$| \Psi \rangle = X_1 | 1 \rangle + X_2 | 2 \rangle , \tag{10}$$

where $| 1 \rangle$ is the space used for the calculation and $| 2 \rangle$ the space which is neglected in our expressions. The complete secular problem is of the form

$$\begin{aligned} H_{11} X_1 + H_{12} X_2 &= E X_1 , \\ H_{21} X_1 + H_{22} X_2 &= E X_2 . \end{aligned} \tag{11}$$

The amplitude X_2 is given by

$$X_2 = \frac{H_{21} X_1}{E - H_{22}} = \frac{\langle 2 | V | 1 \rangle X_1}{E - H_{22}} , \tag{12}$$

and substituting this expression into eq. (11) we obtain the secular problem in space $| 1 \rangle$,

$$\left(H_{11} + \frac{\langle 1 | V | 2 \rangle \langle 2 | V | 1 \rangle}{E - H_{22}} \right) X_1 = E X_1 , \tag{13}$$

with an effective force V^{eff} given in terms of the two-body potential V by the expression

$$V^{\text{eff}} = V + \frac{V | 2 \rangle \langle 2 | V}{E - H_{22}} . \tag{14}$$

A renormalized effective interaction will be a meaningful concept only if the second term is a weakly varying function of the energy E and its numerator does not depend too much on whichever matrix element is calculated. The configuration space $| 1 \rangle$ has been chosen such that the neglected two-quasi-particle and particle-hole states are far away in energy from the lowest computed vibrational states. Likewise the numerators are expected to be small since the neglected single particle states belong to different shells than those of space $| 1 \rangle$ and should have accordingly small overlap with these. However, it is known now that excitations made of more than two quasi-particles do exist at low energy in the region of vibrational states. Whether they bring a strong energy dependent contribution to the effective force renormalization is an open question.

Finally, let us show the expression for the transition rates from the ground state to the excited state $| \Psi \rangle$ when written in the configuration space $| 1 \rangle$ only. The one body transition operator is denoted by θ :

$$\begin{aligned} \langle \Psi | \theta | g \rangle &= X_1 \langle 1 | \theta | g \rangle + X_2 \langle 2 | \theta | g \rangle \\ &= X_1 \left(\langle 1 | \theta | g \rangle + \langle 1 | V | 2 \rangle \frac{1}{E - H_{22}} \times \right. \\ &\qquad \left. \times \langle 2 | \theta | g \rangle \right) \\ &= e^{\text{eff}} \langle 1 | \theta | g \rangle . \end{aligned} \tag{15}$$

This formula shows that the effective charge concept would be reliable only if the second term of the second equation was negligible (this is some sort of rather complicated three-body operator) and if the factor of the first term depend very little upon the denominator as a function of the energy E. We do not know *a priori* whether these two conditions are fulfilled. The effective charge concept will appear to be meaningful here only if practically all of the calculated transition rates are well obtained in the configuration space $| 1 \rangle$, within a unique multiplicative constant. If this is not the case, there is no sound justification for introducing a multiplicative constant or effective charge for the above neglected terms [6]. This is why this calculation will be performed without any effective charge. We assert that the results will be much more meaningful without such a multiplicative factor in the amplitudes. The importance of the space $| 2 \rangle$ will show up in the degree of agreement reached within the space $| 1 \rangle$ alone. As will be shown later, the failure of the present model to describe appropriately the transition properties of even parity states will indicate that the neglected configuration space $| 2 \rangle$ of the present model although not important for odd parity states must play an important role for even parity states.

3. **Results and discussions.** — For clarity it is best to separate the presentation of the results in two parts. First, we shall discuss the general features of the calculated energies and transition rates, and compare them with experiments. All the main points obtained in this work and the assessment of its successes and failures are contained in this general discussion and the casual reader may skip the second part. In the second part, we discuss in detail the shell model structures of the lowest vibrational states as given by the model. This discussion is necessary to show the variety of structures of states generally referred to as *vibrational* as well as to show the complexity of the interplay of core and valence particle configurations throughout the mass table. The results of the calculation are presented in tables III to X and in figures 1 to 4. In table III, the results for the isotones $N = 50$ are discussed in detail, for $J = 2, 3, 4$. There, both the Tamm-Dancoff and Random Phase Approxi-

mations are compared. In tables IV the results are given for all other studied regions, for the $J = 2, 4, 3$ states respectively, but only within the R.P.A. framework. In these tables, we compare the results obtained within the open shell configurations alone with the results obtained when adding to that open shell the particle-hole excitations of the core. The energies and electromagnetic transition rates defined by eqs. (5) and (6) are compared with the available experimental data [7]. The quoted experimental electromagnetic $B(E\lambda)$ are obtained generally from electron inelastic scattering or from Coulomb excitation measurements as extracted from reference [7]. In table V, we compare all calculated electromagnetic, isoscalar and isovector $B(E\lambda)$ for $\lambda = 2$ and 3. The few experimentally known values are given between parenthesis. Tables VI and VII are the wave functions for the lowest 2^+ and 3^- states, calculated with the R.P.A. in the space of valence and core two-quasiparticle configurations. They are given for series of isotopes and isotones (except for the lengthy case of Pb isotopes) for further use in calculating inelastic electron, proton, alpha, etc... form factors.

In figures 1 to 4, we have given the results of the

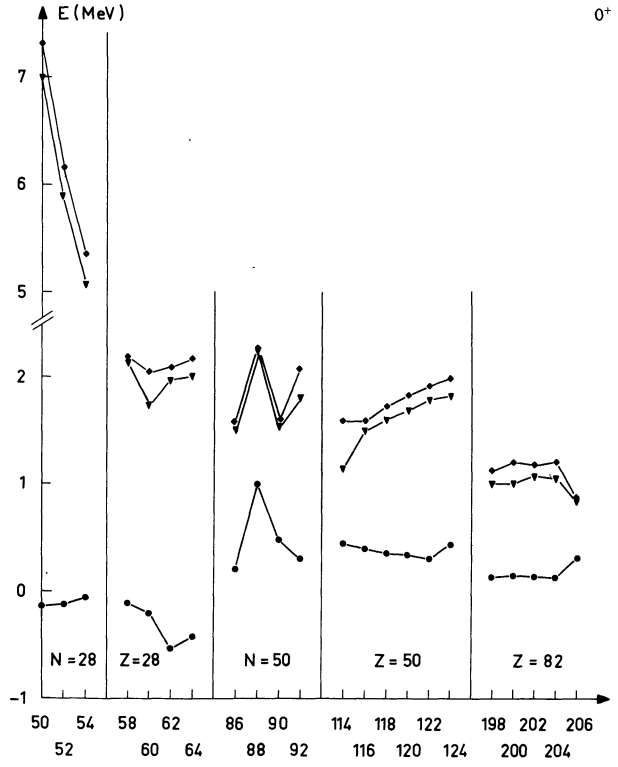

FIG. 1. — The energy for the lowest excited 0^+ state in $N = 28$, $Z = 28$, $N = 50$, $Z = 50$ and $Z = 82$ regions. The square line represents the energy calculated in full space (core and valence configurations), and the triangle line calculated in the valence space alone. The spurious state caused by the non-conservation of number is shown also to show the consistency of the calculational scheme. It should lie exactly at zero energy for a fully consistent calculation. The numbers given under each region stand for the mass number A.

◆ Energy (core + open shell)
▼ Energy (open shell)
} 1st Level
● Spurious state

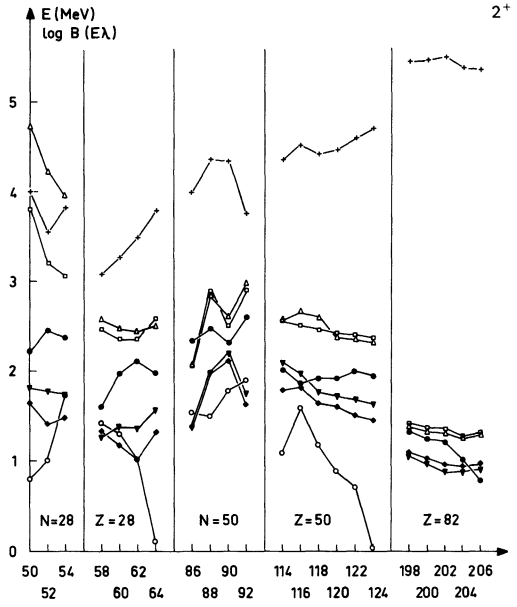

FIG. 2. — The energy and log ($B(E\lambda)$) for the first and second 2^+ states. The legend is indicated. Note that the lowest core state energy is also given. As in figure 1, the mass number is indicated under each region.

◆ Energy (core + open shell)
▼ Energy (open shell)
● log $B(E\lambda)$ (core + open shell)
} 1st Level
□ Energy (core + open shell)
△ Energy (open shell)
○ log $B(E\lambda)$ (core + open shell)
} 2nd Level
+ Energy of the lowest core state

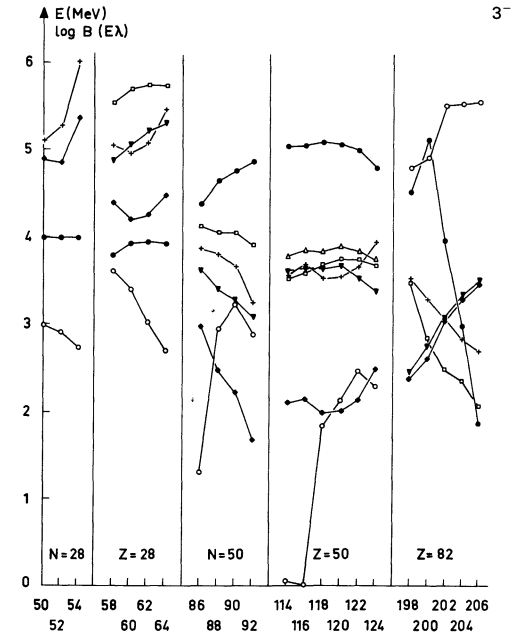

FIG. 3. — The same as figure 2 for the 3^- states :

◆ Energy (core + open shell)
▼ Energy (open shell)
● log $B(E\lambda)$ (core + open shell)
} 1st Level
□ Energy (core + open shell)
△ Energy (open shell)
○ log $B(E\lambda)$ (core + open shell)
} 2nd Level
+ Energy of the lowest core state

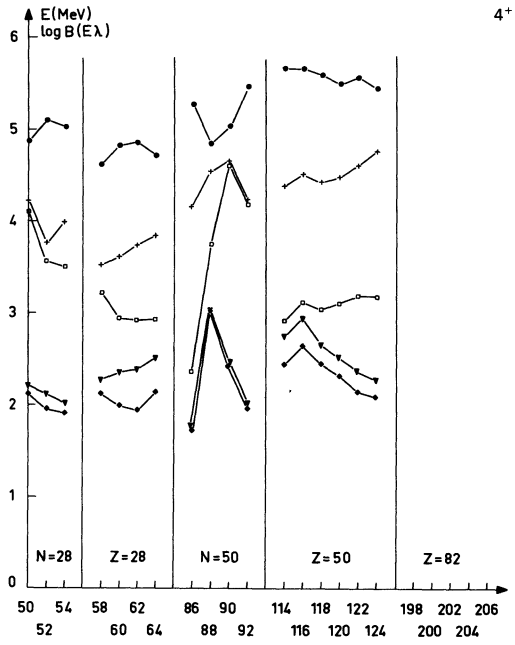

FIG. 4. — The same as figure 2 for the 4^+ states. The $B(E4)$ for the second excited state is not given.

◆ Energy (core + open shell) } 1st Level
▼ Energy (open shell)
● log $B(E\lambda)$ (core + open shell)
□ Energy (core + open shell) 2nd Level
+ Energy of the lowest core state

R.P.A. for the energies of the lowest or two lowest vibrational states calculated with the core excitations. In many cases, we have also shown the states corresponding to the lowest vibrations obtained with the valence particles alone or with the core particles alone (*core states*). On the same figures, we have given the logarithm of the transition rates for the lowest state obtained with and without core polarization. These figures show the variation of the structure and collectivity of vibrational states as a function of mass number A. They will be used essentially in the discussion of subsection 3.2 below.

For all the reasons given above, we consider that to search for an exact fit of the energies is not meaningful. We are rather looking at the overall degree of agreement which can be reached with the model with a minimal manipulation of the parameters. Hence, we have not attempted to vary the few parameters which are left at our disposal by the phenomenological prescriptions we have adopted. As stated before, the $T = 1$, $S = 0$ force strength V_0 is given uniquely by the inverse gap equation analysis of odd A nuclei spectra. The other important component which also acts in even states, namely the $T = 0$, $S = 1$ strength, has been kept to a fixed value throughout the table, i.e. $a = 1.25$ in eq. (3). The other less important odd state components have also been kept fixed to $b = -0.4$ and $c = 1$ in eq. (3), corresponding respectively to the $S = 1$, $T = 1$ and $S = 0$, $T = 0$ components of the force. In any case these two last parameters play a very minor role in spectroscopic fits as compared to the even-state interactions. This for example has been shown extensively for b in the I.G.E. analysis of reference [2]. The value $b = -0.4$ is the one most generally adopted in spectroscopic calculations with effective forces. The parameter c on the other hand is rather undetermined in usual spectroscopic analysis, in particular because of its small statistical weight factor. The range of the gaussian force is 1.7 F and the harmonic oscillator parameters α which were used are given in table II.

TABLE II

The harmonic oscillator parameters $\alpha = (\hbar/m\omega)^{1/2}$ *for each region considered*

Region	$N = 28$	$Z = 28$	$N = 50$	$Z = 50$	$Z = 82$
α (in Fm)	2.0	2.0	2.13	2.27	2.50

Harmonic Oscillator Parameters $\alpha = \sqrt{\hbar/m\omega}$.

3.1 GENERAL FEATURES OF THE RESULTS AND COMPARISON WITH EXPERIMENTS. — 3.1.1 *R.P.A. versus* T.D.A. — In table III, we compare the R.P.A. with the T.D.A. for $N = 50$. As already known, the ground state correlations introduced by the former play a minor role when the configuration space is limited to only two quasi-particles in the outer open shell. There, they modify only slightly the energies and $B(E\lambda)$. This modification is not always an enhancement as can be seen on the results of the 2^+ and 4^+ states of ^{90}Zr and ^{92}Mo. This comes from the fact that two-quasi-particle matrix elements contain contributions from the two-particle interaction which do not have the phase separability which is specific of the particle-hole interaction and which has been shown by the schematic model of Brown and Bolsterli to be responsible for the collective enhancement in the R.P.A. [8]. On the other hand, ground state correlations become important when going to the extended closed core space because of this particle-hole coherence. However here again, one must distinguish between even parity and odd parity states. The effect is quite dramatic for the odd-parity states, but much less so for the even parity states. This can be understood easily. The change of parity when going from one shell to the next one yields a much larger particle-hole configuration space for the odd parity states as compared to the even parity ones (for which the limitation to two major shells only involve the non normal parity sub-shell). As a consequence, the R.P.A. gives a strong collective enhancement in transition rates (by factors of 4 or more) as well as a very large displacement of the energies for the odd parity states when including core excitations. This R.P.A. effect in the case of the odd parity states always improves the results and brings their energies and transition rates close to the experimental values.

3.1.2 *Effect of the particle-hole polarization of the core.* — When comparing in tables III and IV the

TABLE III

Energies and B(Eλ) for the lowest 3^-, 2^+, 4^+ states in N = 50 isotones. Here T.D.A. *and* R.P.A. *are compared for the configuration spaces* : a) *consisting of only 2-quasi-particle states and* b) *consisting of 2-quasi-particle plus core states. Experimental numbers are taken from Bernstein* [7].

		2 Q.P.				2 Q.P. + core					
		T.D.A.		R.P.A.		T.D.A.		R.P.A.		Experiment	
	J^π	E	$B(E\lambda)$	E	$B(E\lambda)$	E	$B(E\lambda)$	E	$B(E\lambda)$	E	$B(E\lambda)$
		—		—		—		—		—	
	3^-	3.63	8 069	3.63	8 525	3.25	14 650	2.97	23 350	3.12	
^{86}Kr	2^+	1.39	184	1.38	193	1.41	194	1.38	221	1.56	
	4^+	1.76	167 000	1.76	172 600	1.77	177 700	1.74	190 100		
	3^-	3.40	12 090	3.39	13 260	2.97	22 130	2.47	43 910	2.74	80 600 ± 3 000
^{88}Sr	2^+	2.01	252	1.99	273	2.06	269	1.99	300	1.83	1 000 ± 200
	4^+	3.04	62 610	3.03	61 260	3.08	71 720	3.05	71 050	4.30	370 000 ± 80 000
	3^-	3.29	13 330	3.28	14 670	2.83	25 080	2.22	57 160	2.74	109 000
^{90}Zr	2^+	2.23	187	2.19	162	2.19	214	2.14	206	2.18	815
	4^+	2.46	73 300	2.45	70 400	2.44	101 500	2.43	106 700	3.09	221 000 ± 55 000
	3^-	3.08	13 200	3.08	14 170	2.55	24 640	1.67	72 620	2.88	
^{92}Mo	2^+	1.77	300	1.75	279	1.70	384	1.64	411	1.54	1 170 ± 200
	4^+	2.02	186 200	2.02	182 900	1.99	261 300	1.96	295 000	2.33	

energies obtained with and without core particle-hole excitations, one finds as just stated above that the core plays a small role for the low-lying even parity vibrations but is essential for the odd-parity octupole ones. Nevertheless the effect of the core for even parity states is larger than it appears at first sight. Let us recall that in the framework of the I.G.E. phenomenology, the effective interaction strength given by that method gets reduced by almost twenty per cent when the core is open, as shown and discussed in detail in reference [2]. The meaning of this effect is obvious : the larger the configuration space, the smaller is the effective force renormalization. Now it is seen that the core configuration mixing in even parity states is sufficient to compensate for this reduction of the force strength and that it yields energies as low or even lower by several hundred keV as compared to the valence particle configurations alone. In the case of the octupole states, core excitations make up almost all the structure, as expected from the parity jump between adjacent shells. In this case obviously the particle-hole core polarization cannot be treated as perturbative, as it has been sometimes done in the past.

3.1.3 *Discussion of the energies.* — We comment first on the position of the spurious states : the dipole spurious state which results from the C.M. motion and the monopole spurious state due to the particle number violation in the B.C.S. approximation. Their positions in the R.P.A. calculation are of some interest since according to Thouless' theorem [9] they should come at zero energy in a completely self-consistent treatment. Hence their deviation from this value is an indication of the degree of inconsistency of this semi-phenomenological calculation. The position of the spurious dipole state for example varies between 0.1 MeV for ^{86}Kr up to an imaginary value, $4i$ MeV for ^{94}Tc, from $2.7i$ in ^{198}Pb up to $3.55i$ in ^{206}Pb. Of course these values have a very limited meaning since they would be extremely sensitive to parameter variations (if we had chosen to vary any) because of the strongly collective character of the spurious states. The spurious 0^+ state is shown in figure 1. Its energy is close to zero or slightly imaginary (in this figure, this is represented by a negative value). For the $N = 28$ and $Z = 28$ cases, this value is seen to be smaller than $0.25i$ MeV, while it is real and positive for all other regions and inferior to 0.5 MeV except for the case of ^{88}Sr.

We turn to the energies of the physical states. It is seen that the agreement with experiment is rather good for all nuclei. This is all the more satisfactory considering the strict rules adopted to fix the parameters. For all nuclei and for all states except in very rare instances the agreement is better than 0.5 MeV. The main exceptions are the 3^- state of ^{92}Mo and the 4^+ state of ^{88}Sr. They are among the nuclei for which there are some uncertain identifications of the particle-hole input energies. The inclusion of the core always improves the agreement with the experiment. In particular, this inclusion plays a sizable role for the nickel and tin isotopes, and is even essential for some 3^- states like those of the $N = 28$ isotones. The inclusion of core particle-hole excitations thus permits to obtain an overall rough agreement for the 3^-, 2^+ and 4^+ lowest vibrations in a same nucleus and for all S.C.S. nuclei.

3.1.4 *Discussion of the transition rates.* — These general agreements obtained for energies indicate really that the crucial test of the model will lie in its

ability to describe the transition properties. Hence we shall now consider the electromagnetic $B(E\lambda)$. Strictly speaking, the e.m. transition rates for isotopes calculated with only the outer shell nucleons should vanish as indicated in table IV, and for these nuclei the introduction of core particle-hole configurations is of course essential as it is the simplest way of bringing in proton components. However for demonstration purposes we have indicated between parenthesis and only in the case of the tin isotopes the $B(E\lambda)$ which would be obtained when giving an effective charge of one to the neutrons. In table III, we also note that the effect on the 3^- transition rates of the Random Phase Approximation is extremely large. The R.P.A. always brings in very large enhancement factors.

TABLE IV*a*

Same as table III (*but* R.P.A. *only*) *for other regions* : i.e. $N = 28$, $Z = 28$, $Z = 50$, $Z = 82$

	3^- Valence particle E	$B(E\lambda)$	3^- Valence + core particle E	$B(E\lambda)$	Experiment E	$B(E\lambda)$
	—		—		—	
^{50}Ti	8.40	0.20×10^4	4.88	0.95×10^4	4.42	
^{52}Cr	7.94	0.43×10^4	4.85	0.93×10^4	4.59	$.91 \times 10^4$
^{54}Fe	7.78	0.61×10^4	5.36	0.94×10^4	4.76	$.95 \times 10^4$
^{58}Ni	4.88	0	4.39	0.60×10^4	4.47	0.14×10^5
^{60}Ni	5.05	0	4.19	0.81×10^4	4.04	0.21×10^5
^{62}Ni	5.21	0	4.24	0.86×10^4	3.75	
^{64}Ni	5.30	0	4.47	0.80×10^4		
$N = 50$ see table III						
^{114}Sn	3.58	0 (0.12)	2.11	1.11×10^5	2.30	
^{116}Sn	3.65	0 (0.10)	2.14	1.13	2.24	1.20×10^5
^{118}Sn	3.65	0 (0.27)	1.98	1.22	2.30	1.10×10^5
^{120}Sn	3.68	0 (0.34)	2.01	1.18	2.40	1.13×10^5
^{122}Sn	3.53	0 (0.38)	2.14	0.97	2.50	
^{124}Sn	3.38	0 (0.24)	2.49	0.63	2.53	0.76×10^5
^{198}Pb	2.46	0	2.38	0.33×10^5		
^{200}Pb	2.76	0	2.61	0.13×10^6		
^{202}Pb	3.08	0	2.49	0.32×10^6		
^{204}Pb	3.34	0	2.36	0.34×10^6	2.6	
^{206}Pb	3.50	0	2.07	0.35×10^6	2.65	

TABLE IV*b*

	2^+ Valence particle E	$B(E\lambda)$	2^+ Valence + core particle E	$B(E\lambda)$	Experiment E	$B(E\lambda)$
	—		—		—	
^{50}Ti	1.81	0.11×10^3	1.64	0.16×10^3		
^{52}Cr	1.78	0.17×10^3	1.41	0.23×10^3	1.43	0.48×10^3
^{54}Fe	1.74	0.13×10^3	1.48	0.24×10^3	1.41	0.49×10^3
^{58}Ni	1.27	0	1.32	0.39×10^2	1.45	0.70×10^3
^{60}Ni	1.37	0	1.18	0.93×10^2	1.33	0.10×10^4
^{62}Ni	1.37	0	1.01	0.13×10^3		
^{64}Ni	1.55	0	1.32	0.97×10^2		
$N = 50$ see table III						
^{114}Sn	2.10	0 (892)	1.79	102	1.26	$2\,300 \pm 500$
^{116}Sn	1.97	0 (760)	1.83	73	1.27	$2\,120 \pm 250$
^{118}Sn	1.79	0 (1 003)	1.65	82	1.22	$2\,300 \pm 270$
^{120}Sn	1.74	0 (988)	1.61	83	1.18	$2\,200 \pm 220$
^{122}Sn	1.69	0 (1 476)	1.51	101	1.14	$2\,500 \pm 300$
^{124}Sn	1.65	0 (1 492)	1.47	89	1.13	$2\,150 \pm 240$
^{198}Pb	1.07	0	1.10	0.21×10^2		
^{200}Pb	0.99	0	1.03	0.18×10^2		
^{202}Pb	0.90	0	0.98	0.17×10^2		
^{204}Pb	0.90	0	0.96	0.10×10^2		
^{206}Pb	0.93	0	0.98	0.63×10^1		

TABLE IV*c*

	4^+ Valence particle E	$B(E\lambda)$	4^+ Valence + core particle E	$B(E\lambda)$	Experiment E	$B(E\lambda)$
	—		—		—	
^{50}Ti	2.20	0.51×10^5	2.12	0.74×10^5	2.66	
^{52}Cr	2.11	0.77×10^5	1.95	0.13×10^6	2.31	
^{54}Fe	2.01	0.61×10^5	1.90	0.11×10^6	2.56	
^{58}Ni	2.27	0	2.12	0.41×10^5	2.46	
^{60}Ni	2.35	0	1.99	0.67×10^5	(2.16)	
^{62}Ni	2.38	0	1.94	0.73×10^5	(2.30)	
^{64}Ni	2.50	0	2.13	0.53×10^5	(2.62)	
$N = 50$ see table III						
^{114}Sn	2.75	0	2.45	0.47×10^6		
^{116}Sn	2.95	0	2.65	0.47×10^6		
^{118}Sn	2.67	0	2.46	0.40×10^6		
^{120}Sn	2.53	0	2.33	0.33×10^6		
^{122}Sn	2.39	0	2.16	0.38×10^6		
^{124}Sn	2.29	0	2.10	0.28×10^6		

Comparison with experiment shows two different situations :

a) The experimentally observed strength of the 3^- transitions can always be mostly accounted for by contributions from the simple core particle-hole configurations. This is the case both in isotopes where the core states are the only ones to participate in the electromagnetic transition and in isotones where these core contributions add up coherently to those of the open shell protons. The agreement with experiment is well within a factor of two for all octupole states from the lightest to the heaviest nuclei. Such agreements should be considered as excellent, in view of the well known limitations of a shell model calculation which uses harmonic oscillators, severely truncates the configuration space and introduces experimental quasi-particle energies, as discussed in section 2.

b) For even parity states, we must distinguish between isotones and isotopes. The agreement in isotones is not bad, that is within a factor of 2 to 3, similar to the agreements reached in the case of the 3^-. On the contrary, the electromagnetic transition rates for the even-parity states of isotopes are always far from being explained by the model. Even if we exhaust all significant simple core particle-hole configurations as well as the open shell two quasi-particle ones, the disagreement between experimental and theoretical values are very large, from factors of 5 to factors of 1 or 2 orders of magnitudes. Thus, considering the agreement with energies, it can clearly be stated that a mechanism is missing in the present description essential for the electromagnetic transitions for the even parity states while unimportant for the energies.

In fact, even if the calculation had been carried out in a single isotope region, and the force strength had been varied for a perfect agreement for energies, such an adjustment of parameters could not have accounted by any means for the missing transition strength in even parity states. This is all the more serious considering the good agreement obtained for the octupole states and the fair agreement obtained for 2^+ and 4^+ transitions in isotones.

3.1.5 *Comparison of electromagnetic, isoscalar and isovector transition rates.* — In table V, we compare the predicted $B(E\lambda)$ not only for electromagnetic transition rates but also for the $\Delta T = 0$ and $\Delta T = 1$ cases (see eq. (7)). The e.m. operator projects onto the proton particle-hole components and proton two quasi-particle components (in the case of isotones) while the $\Delta T = 0$ operator is just the isoscalar part of the e.m. operator and involves all nucleons in both core and open shells. *A priori* one would expect the two transitions to be of rather different magnitude in isotopes since, in this case, only the core particles contribute to the electromagnetic transitions while both the core and the open shell particles cooperate in the $\Delta T = 0$ transitions. As can be seen in table V, this effect does exist but is not large. The isoscalar transitions are enhanced only by a factor of 2 as compared to the electromagnetic ones. Of course this effect is smaller for isotones; in fact in many cases it is almost negligible. These calculated transitions explain somewhat the similarities which have often been observed between the $B(E\lambda)$ extracted from electromagnetic and α-scattering experiments. For example, let us compare the 3^- and 2^+ $B(E\lambda)$ in tin isotopes, see figure 5. There the 3^- e.m. transition results from the contribution of a single core vibration whose energy is merely shifted by its interaction with two-quasi-particle configurations. On the other hand, the $\Delta T = 0$ transitions result from coherent contributions of this core vibration and the outer particles,

TABLE V

Reduced matrix elements $B(E2)$ and $B(E3)$ for e.m., $\Delta T = 0,1$ *transitions calculated in* R.P.A. *The experimental values, when known, are given between parenthesis. They are taken from reference* [7]

	2^+			3^-		
	e	$\Delta T = 0$	$\Delta T = 1$	e	$\Delta T = 0$	$\Delta T = 1$
	—	—	—	—	—	—
^{50}Ti	0.17×10^3	0.10×10^3	0.72×10^2	0.95×10^4	0.13×10^5	0.25×10^3
^{52}Cr	0.23×10^3	0.19×10^3	0.11×10^2	0.93×10^4	0.13×10^5	0.27×10^3
	(0.48×10^3)	(0.44×10^3)		$(.91 \times 10^4)$	(0.46×10^4)	
^{54}Fe	0.24×10^4	0.14×10^3	0.11×10^2	0.94×10^4	0.12×10^5	0.16×10^3
	(0.49×10^3)	(0.35×10^3)		$0.95 \times 10^4)$	(0.31×10^4)	
^{58}Ni	0.39×10^2	0.14×10^3	0.31×10^2	0.60×10^4	0.10×10^5	0.59×10^3
	(0.70×10^3)	(0.11×10^4)		(0.14×10^5)	(0.22×10^5)	
^{60}Ni	0.93×10^2	0.30×10^3	0.60×10^2	0.81×10^4	0.13×10^5	0.58×10^3
	(0.10×10^4)	(0.14×10^4)		(0.21×10^5)	(0.25×10^5)	
^{62}Ni	0.13×10^3	0.42×10^3	0.84×10^2	0.86×10^4	0.13×10^5	0.52×10^3
					(0.19×10^5)	
^{64}Ni	0.97×10^2	0.30×10^3	0.55×10^2	0.80×10^4	0.13×10^5	0.56×10^3
^{86}Kr	0.22×10^3	0.92×10^2	0.28×10^2	0.23×10^5	0.24×10^5	0.40×10^3
^{88}Sr	0.30×10^3	0.13×10^3	0.34×10^2	0.44×10^5	0.38×10^5	0.23×10^3
	(0.10×10^4)			(0.80×10^5)		
^{90}Zr	0.21×10^3	0.86×10^2	0.26×10^2	0.57×10^5	0.47×10^5	0.51×10^3
	(0.42×10^3)	(0.70×10^3)		(0.11×10^6)	(0.66×10^5)	
^{92}Mo	0.41×10^3	0.18×10^3	0.49×10^2	0.73×10^5	0.66×10^5	0.15×10^3
	(0.11×10^4)	(0.96×10^3)			(0.63×10^5)	
^{114}Sn	0.10×10^3	0.57×10^3	0.19×10^3	0.11×10^6	0.11×10^6	0.30×10^1
	(0.23×10^4)					
^{116}Sn	0.73×10^2	0.45×10^3	0.16×10^3	0.11×10^6	0.11×10^6	0.13×10^2
	(0.21×10^4)			(0.83×10^5)	(0.35×10^6)	
^{118}Sn	0.84×10^2	0.56×10^3	0.21×10^3	0.12×10^6	0.11×10^6	0.13×10^3
	(0.23×10^4)			(0.10×10^6)		
^{120}Sn	0.82×10^2	0.58×10^3	0.22×10^3	0.12×10^6	0.11×10^6	0.21×10^3
	(0.22×10^4)			(0.10×10^6)		
^{122}Sn	0.10×10^3	0.74×10^3	0.30×10^3	0.97×10^5	0.87×10^5	0.28×10^3
	(0.25×10^4)					
^{124}Sn	0.89×10^2	0.69×10^3	0.28×10^3	0.63×10^5	0.53×10^5	0.40×10^3
	(0.22×10^4)			(0.76×10^5)		

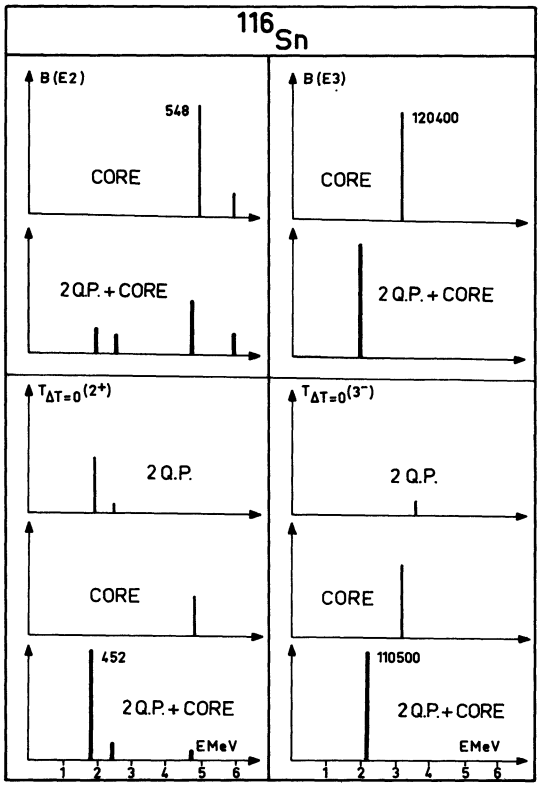

FIG. 5. — Core-coupling effect on e.m. and $\Delta T = 0$ transition rates. The relative values of the reduced matrix elements squared of the e.m. and $\Delta T = 0$ operators are given as ordinates. These values were calculated in R.P.A. limited : *a*) to the p-h configurations of the core (CORE); *b*) to the external two-quasiparticle configurations (2 Q.P.); *c*) to the complete 2 Q.P. and p-h core space (2 Q.P. + CORE). The absolute values are given next to the most important strengths, in units of $e^2 F^{2\lambda}$ for $B(E\lambda)$ and $F^{2\lambda}$ for $T_{\Delta T=0}$.

which by themselves alone would yield a single two-quasi-particle vibration in the considered energy region. The situation is very different for the 2^+ states. Several 2^+ states are excited by the electromagnetic and $\Delta T = 0$ operators, since there is not just one collective core state of even parity but rather many core states of almost pure one particle-one hole nature. The strength of the core states are depleted by the low-lying two-quasi-particle states. There is a clear difference between the two types of transitions : in the $\Delta T = 0$ case there is a concentration of strength in the lowest two-quasi-particle states due to a coherent enhancement of the core and external shell contributions, whereas in the electromagnetic case no such enhancements can occur since the neutron quasi-particles do not contribute. This explains why large e.m. $B(E2)$ are difficult to obtain in this simple configuration space while larger theoretical enhancements can be obtained for the $\Delta T = 0$ transitions even with the addition of only a small number of core particle-hole configurations. In the case of isotones the situation is different. Now for both the e.m. and $\Delta T = 0$ transitions, there is a coherent enhancement due to the interplay of the core and the outer shell proton contributions. It is interesting to note that in this case the electromagnetic $B(E\lambda)$ are always larger than the $\Delta T = 0$ ones.

Let us note that the experimental $B(E\lambda)$ observed in the Ni isotopes are very similar both for e.m. and $\Delta T = 0$ transitions, while the present calculation gives much larger $\Delta T = 0$ transitions, for the reasons just discussed.

The above results are also confirmed by electron, proton and alpha scattering cross-sections computed with the present wave functions. It is found in all these works [10, 11, 12] that the agreement reached for octupole states is impressively good, while the transition strengths for even parity states are in general too low, and much more so for isotopes than for isotones.

In conclusion, on one hand, the energies and transition rates of the odd parity octupole states of single-closed shell nuclei can apparently be understood in terms of particle-hole excitations of the core as was the case with the doubly magic nuclei. On the other hand, in spite of the agreement obtained for the energies, the even parity states of the S.C.S. nuclei appear generally to be of a more complicated nature than that given by this model.

3.2 DETAILED DISCUSSION OF THE SHELL MODEL STRUCTURE OF THE CALCULATED STATES. — The discussion below is essentially related to figures 1 to 4 and to the wave function tables VI and VII. As we have emphasized before, our aim is an overall picture rather than a detail fit, so the discussion, although detailed, will be kept somewhat qualitative. All these results are calculated in the R.P.A. framework. For the purpose of the discussion we shall call *core states* the states obtained with core configurations alone, *open shell states* those obtained with the open shell configurations alone. The orders of magnitude quoted for the $B(E\lambda)$'s, are given in $e^2 F^{2\lambda}$ units, and for the electromagnetic, $\Delta T = 0$ and $\Delta T = 1$ transitions respectively in that order unless otherwise indicated.

3.2.1 0^+ *States.* — As shown in figure 1, apart from the spurious state discussed above, the lowest 0^+ state is dominated, for all the nuclei we have been studying, by a single open-shell configuration. The admixtures of other open-shell or of core configurations are small. It may seem paradoxical that the dominant state obtained with open-shell configurations alone lies at a lower energy than the state with core configurations. Of course admixtures normally lower the lowest state. Here this happens simply because of the modification of the strength of the effective force which, as already discussed in a previous paper, decreases when the number of orbitals in the gap equations is increased.

3.2.1.1 $N=28$ isotones. — The lowest physical 0^+ state is very high-lying. It is almost purely a $(p\ 3/2)^2$ proton two-quasi-particle configuration. The decrease of its excitation energy from 7.3 MeV in ^{50}Ti to 5.3 MeV is a simple consequence of the filling of the

TABLE VI

R.P.A. *wave functions for the lowest 2^+ state. A stands for the mass number, E the lowest 2^+ state energy, and the configurations are labelled by the numbers as given in table* I. *The three different configuration spaces are separated by the double vertical lines. The first space corresponds to the valence (quasi-particle) states, the second to the core configurations of the same charge as the valence ones, and the third to the closed core (particle-hole) configurations. The upper and lower entries correspond respectively to the X and Y components* [*see eq.* (4)].

$N = 28$ isotones $J^\pi = 2^+$

A	E	7/7	8/8	9/9	11/11	7/8	7/9	8/9	8/10	9/10	11/4	6/6	4/4	6/5	6/4	5/4	8/7	9/7	11/4
50	1.64	− 0.945	− 0.029	− 0.078	− 0.034	0.191	− 0.107	0.030	− 0.035	0.045	− 0.043	− 0.013	− 0.004	− 0.009	0.009	0.007	0.241	0.063	− 0.075
		− 0.060	− 0.001	0.001	0.001	0.032	− 0.014	0.002	− 0.000	0.002	− 0.030	0.025	0.013	0.022	− 0.019	− 0.020	0.104	0.045	− 0.057
52	1.41	0.910	0.029	0.062	0.028	− 0.246	0.102	− 0.029	0.032	− 0.043	0.055	0.024	0.008	0.016	− 0.016	− 0.013	− 0.349	− 0.087	0.096
		0.106	0.001	− 0.007	− 0.003	− 0.068	0.027	− 0.002	− 0.001	− 0.001	0.040	− 0.012	− 0.008	− 0.012	0.009	0.012	− 0.153	− 0.065	0.074
54	1.48	0.935	0.020	0.039	0.016	− 0.228	0.083	− 0.020	0.023	− 0.031	0.045	0.032	0.011	0.022	− 0.023	− 0.019	− 0.280	− 0.071	0.080
		0.068	− 0.006	− 0.029	− 0.011	− 0.063	0.025	0.004	− 0.011	0.010	0.032	− 0.004	− 0.004	− 0.005	0.004	0.005	− 0.121	− 0.052	0.061

Nickel isotopes $J^\pi = 2^+$

A	E	8/8	9/9	11/11	8/9	8/10	9/10	8/7	9/7	11/4	4/5	4/6	5/6	4/4	6/6	7/7	8/7	9/7	11/4
58	1.32	− 0.729	− 0.180	− 0.044	0.166	− 0.556	0.200	0.183	0.036	− 0.041	0.	− 0.004	− 0.001	− 0.003	− 0.006	− 0.012	0.190	0.058	− 0.058
		− 0.040	− 0.014	0.002	0.025	− 0.048	0.016	0.039	0.033	− 0.024	− 0.009	0.007	− 0.008	0.009	0.009	0.028	0.098	0.044	− 0.045
60	1.18	0.518	0.290	0.052	− 0.228	0.590	− 0.363	− 0.265	− 0.072	0.063	− 0.005	0.007	− 0.004	0.007	0.011	0.046	− 0.282	− 0.093	0.090
		0.061	0.043	− 0.006	− 0.050	0.081	− 0.072	− 0.068	− 0.046	0.042	0.008	− 0.005	0.005	− 0.007	− 0.005	− 0.012	− 0.163	− 0.069	0.072
62	1.01	0.387	0.380	0.045	− 0.254	0.531	− 0.475	− 0.315	− 0.098	0.075	− 0.016	0.011	− 0.014	0.011	0.016	0.092	− 0.314	− 0.104	0.108
		0.074	0.092	− 0.016	− 0.065	0.104	− 0.120	0.101	− 0.047	0.055	0.001	− 0.001	− 0.002	− 0.003	0.001	0.018	− 0.201	− 0.081	0.090
64	1.32	0.306	0.414	0.031	− 0.248	0.469	− 0.548	− 0.294	− 0.090	0.066	− 0.019	0.013	− 0.016	0.014	0.017	0.104	− 0.300	− 0.086	0.093
		0.044	0.063	− 0.032	− 0.039	0.094	− 0.086	− 0.054	− 0.024	0.048	0.	0.	− 0.003	− 0.001	0.001	0.017	− 0.155	− 0.066	0.075

TABLE VI *(suite)*

$N = 50$ isotones $J^\pi = 2^+$

A	E	11/11	9/9	8/8	10/9	10/8	9/8	11/12	11/13	12/13	12/14	13/14	13/15	14/15	12/12	13/13	14/14	16/16	13/11	12/11
86	1.38	− 0.033	− 0.169	− 0.879	0.135	0.362	− 0.182	− 0.007	0.032	− 0.005	0.013	− 0.012	0.007	− 0.005	− 0.009	− 0.016	− 0.010	− 0.005	0.138	0.020
		0.016	0.014	− 0.018	0.026	0.023	− 0.007	0.004	− 0.012	0.001	− 0.007	0.007	− 0.004	0.003	0.006	0.006	0.005	0.005	0.063	0.018
88	1.99	− 0.065	− 0.116	− 0.449	0.348	0.784	− 0.119	− 0.006	0.041	− 0.004	0.011	− 0.006	0.007	− 0.005	− 0.007	− 0.014	− 0.006	− 0.005	0.196	0.028
		0.027	0.007	− 0.010	0.024	0.058	− 0.001	0.005	− 0.024	0.004	− 0.012	0.009	− 0.007	0.005	0.009	0.013	0.008	0.007	0.064	0.023
90	2.14	− 0.916	− 0.041	− 0.089	0.157	0.306	− 0.030	− 0.045	0.103	− 0.008	0.023	− 0.011	0.018	− 0.011	− 0.040	− 0.015	− 0.009	− 0.014	0.146	0.023
		0.009	0.048	0.015	− 0.016	− 0.004	0.014	0.001	− 0.009	0.002	− 0.006	0.004	− 0.004	0.003	0.006	0.007	0.004	0.004	0.048	0.018
92	1.64	− 0.948	− 0.038	− 0.070	0.089	0.183	− 0.025	− 0.046	0.121	− 0.008	0.023	− 0.009	0.016	− 0.010	− 0.037	− 0.012	− 0.008	− 0.013	0.203	0.034
		− 0.019	0.029	0.006	− 0.002	0.005	0.008	− 0.003	0.012	0.001	− 0.005	0.004	− 0.004	0.002	0.009	0.006	0.004	0.005	0.085	0.027

Sn isotopes $J^\pi = 2^+$

A	E	12/12	13/13	14/14	16/16	12/13	12/14	13/14	13/15	14/15	11/11	9/9	8/8	12/11	13/11	10/9	10/8	9/8	12/11	13/11
114	1.79	0.387	0.138	0.180	0.213	0.094	− 0.511	0.112	− 0.412	0.472	0.032	0.010	0.010	− 0.025	− 0.086	− 0.010	− 0.014	0.005	− 0.055	− 0.291
		0.003	− 0.010	− 0.008	− 0.021	0.006	− 0.046	0.026	− 0.025	0.017	− 0.609	− 0.006	− 0.005	0.001	0.007	0.005	0.007	− 0.002	− 0.042	− 0.111
116	1.83	− 0.186	− 0.093	− 0.276	− 0.272	− 0.052	0.424	− 0.097	0.331	− 0.672	− 0.023	− 0.008	− 0.008	0.017	0.065	0.008	0.012	− 0.009	0.046	0.245
		0.015	0.018	0.004	0.013	− 0.001	0.040	− 0.024	0.016	− 0.020	0.010	0.007	0.005	− 0.006	− 0.011	− 0.005	− 0.008	0.002	0.036	0.094
118	1.65	0.172	0.113	0.360	0.380	0.053	− 0.381	0.132	− 0.314	0.601	0.028	0.011	0.012	− 0.022	− 0.080	− 0.010	− 0.017	0.005	− 0.059	− 0.25
		− 0.012	− 0.010	0.007	− 0.007	0.003	− 0.034	0.014	− 0.020	0.020	− 0.009	− 0.007	− 0.004	0.005	0.005	0.005	0.007	− 0.002	− 0.043	− 0.110
120	1.61	0.168	0.119	0.383	0.457	0.052	− 0.346	0.142	− 0.300	0.560	0.032	0.013	0.015	− 0.026	− 0.087	− 0.012	− 0.020	0.006	− 0.065	− 0.242
		− 0.009	− 0.004	0.010	− 0.002	0.003	− 0.027	0.007	− 0.021	0.019	− 0.007	− 0.007	− 0.003	0.005	0.002	0.004	0.005	− 0.001	− 0.045	− 0.113
122	1.51	− 0.188	− 0.118	− 0.349	− 0.583	− 0.053	0.346	− 0.140	0.272	− 0.461	− 0.035	− 0.016	− 0.015	0.033	0.091	0.014	0.021	− 0.007	0.074	0.260
		− 0.003	0.	− 0.014	− 0.034	− 0.006	0.042	− 0.015	0.023	− 0.025	0.005	0.005	0.002	− 0.002	0.004	− 0.003	− 0.004	0.001	0.052	0.130
124	1.47	− 0.216	− 0.123	− 0.326	− 0.639	− 0.056	0.345	− 0.141	0.257	− 0.403	− 0.041	− 0.020	− 0.016	0.040	0.097	0.017	0.023	− 0.008	0.074	0.239
		− 0.015	− 0.004	− 0.013	− 0.043	− 0.007	0.044	− 0.017	0.021	− 0.026	− 0.001	0.002	0.001	0.003	0.009	− 0.001	− 0.002	− 0.	0.052	0.125

TABLE VII

Same as table VI *for the lowest* 3^- *state*

$N = 28$ isotones $J^\pi = 3^-$

A	E	7/11	8/11	9/11	7/6	7/5	7/4	8/6	8/4	9/6	9/5	9/4	10/4	8/6	8/4	9/6	9/5	9/4	10/4	11/7
50	4.88	− 0.223	0.033	0.020	− 0.218	0.315	− 0.169	0.196	0.089	− 0.158	− 0.167	0.081	− 0.082	0.517	0.151	− 0.326	− 0.377	0.115	− 0.158	− 0.398
		− 0.046	0.003	0.003	+ 0.055	− 0.093	+ 0.068	− 0.066	− 0.039	+ 0.060	+ 0.068	− 0.035	+ 0.037	0.080	0.049	− 0.077	− 0.094	0.051	− 0.055	− 0.100
52	4.85	− 0.332	0.046	0.026	− 0.181	0.250	− 0.132	0.199	0.087	− 0.154	− 0.157	0.076	− 0.080	0.495	0.149	− 0.317	− 0.371	0.113	− 0.155	− 0.433
		− 0.067	0.004	0.003	+ 0.040	− 0.069	+ 0.051	− 0.062	− 0.037	+ 0.056	+ 0.064	− 0.033	+ 0.035	0.074	0.046	− 0.071	− 0.088	0.047	− 0.051	− 0.096
54	5.36	− 0.451	0.046	0.026	− 0.150	0.192	− 0.094	0.203	0.083	− 0.157	− 0.152	0.073	− 0.081	0.433	0.138	− 0.288	− 0.346	0.106	− 0.145	− 0.470
		− 0.074	0.002	0.002	+ 0.023	− 0.040	+ 0.030	− 0.053	− 0.031	+ 0.050	+ 0.055	− 0.030	+ 0.032	0.059	0.039	− 0.058	− 0.072	0.040	− 0.043	− 0.084

Nickel isotopes $J^\pi = 3^-$

A	E	8/11	9/11	8/4	8/6	9/4	9/5	9/6	10/4	11/7	4/7	5/7	6/7	8/4	8/6	9/4	9/5	9/6	10/4	11/7
58	4.39	− 0.731	− 0.105	− 0.070	− 0.246	− 0.068	0.216	0.210	0.079	0.305	0.006	− 0.042	− 0.000	− 0.073	− 0.187	− 0.067	0.219	0.166	0.073	0.310
		− 0.037	− 0.007	− 0.019	− 0.037	− 0.024	0.044	0.045	0.026	0.068	− 0.004	0.007	0.000	+ 0.033	+ 0.052	+ 0.031	− 0.060	− 0.050	− 0.037	− 0.076
60	4.19	− 0.659	− 0.150	− 0.067	− 0.211	− 0.077	0.235	0.216	0.079	0.344	0.018	− 0.067	− 0.020	− 0.077	− 0.210	− 0.076	0.252	0.197	0.075	0.367
		− 0.055	− 0.014	− 0.015	− 0.036	− 0.027	0.048	0.052	0.023	0.081	0.003	− 0.004	− 0.008	+ 0.038	+ 0.061	+ 0.037	− 0.069	− 0.059	− 0.042	− 0.091
62	4.24	− 0.631	− 0.205	− 0.067	− 0.206	− 0.064	0.022	0.187	0.078	0.362	0.026	− 0.087	− 0.029	− 0.077	− 0.239	− 0.074	0.258	0.206	0.079	0.372
		− 0.060	− 0.026	− 0.017	− 0.034	− 0.022	0.037	0.045	0.018	0.083	0.009	− 0.010	− 0.013	+ 0.038	+ 0.063	+ 0.036	− 0.069	− 0.060	− 0.042	− 0.092
64	4.47	0.669	0.238	0.052	0.160	0.039	0.152	− 0.117	− 0.088	− 0.378	− 0.021	0.073	0.023	0.075	0.229	0.070	− 0.252	− 0.190	− 0.073	− 0.376
		0.069	0.040	0.011	0.024	0.011	− 0.018	− 0.027	− 0.025	− 0.081	− 0.008	0.008	0.011	− 0.037	− 0.059	− 0.033	+ 0.062	+ 0.053	+ 0.040	+ 0.085

TABLE VII *(suite)*

$N = 50$ isotones $J^\pi = 3^-$

A	E	11/9	11/8	11/16	10/13	10/12	9/12	9/13	9/14	8/12	8/13	8/14	12/16	13/16	9/15	16/11	15/9	14/9	14/8	13/10	13/9	13/8	12/10	12/9	12/8
86	2.97	0.160	−0.788	0.020	−0.090	−0.062	0.125	0.078	−0.069	−0.086	0.189	0.153	−0.002	−0.020	−0.062	0.100	0.097	−0.071	−0.165	0.363	−0.104	0.240	−0.138	0.118	0.066
		0.045	−0.085	0.004	−0.019	−0.011	0.048	0.032	−0.028	−0.019	0.047	0.045	−0.001	−0.003	−0.029	−0.054	−0.033	+0.030	+0.059	−0.079	+0.029	−0.063	+0.051	−0.052	−0.027
88	2.47	−0.160	0.807	−0.020	0.153	0.099	−0.127	−0.072	0.064	0.097	−0.193	−0.158	0.002	0.014	0.079	−0.128	−0.086	0.078	0.184	−0.307	0.100	−0.240	0.169	−0.145	−0.086
		−0.063	0.146	−0.007	0.050	0.029	−0.061	−0.043	0.037	0.029	−0.074	−0.066	0.001	0.003	0.044	+0.075	+0.042	−0.041	−0.084	+0.102	−0.040	+0.086	−0.074	+0.074	+0.040
90	2.22	−0.143	0.809	−0.044	0.235	0.148	−0.120	−0.064	0.058	0.095	−0.182	−0.153	0.003	0.011	0.062	−0.143	−0.083	0.079	0.186	−0.295	0.096	−0.230	0.191	−0.163	−0.098
		−0.066	0.174	−0.022	0.089	0.050	−0.066	−0.045	0.039	0.035	−0.086	−0.075	0.001	0.001	0.043	+0.089	+0.047	−0.047	−0.098	+0.118	−0.045	+0.099	−0.090	+0.089	+0.049
92	1.67	0.114	−0.784	0.100	−0.250	−0.163	0.126	0.066	−0.060	−0.102	0.209	0.174	−0.006	−0.016	−0.064	0.168	0.105	−0.104	−0.250	0.350	−0.112	0.276	−0.213	0.188	0.110
		0.065	−0.236	0.060	−0.123	−0.075	0.084	0.048	−0.044	−0.051	0.117	0.105	−0.003	−0.002	−0.048	−0.118	−0.065	+0.065	+0.146	−0.171	+0.061	−0.143	+0.123	−0.120	−0.065

Sn isotopes $J^\pi = 3^-$

A	E	12/16	13/16	12/10	12/9	12/8	13/10	13/9	13/8	14/9	14/8	15/9	16/11	11/9	11/8	12/10	12/9	12/8	13/10	13/9	13/8	14/9	14/8	15/9	16/11
114	2.10	−0.290	−0.697	−0.078	0.069	0.047	0.044	−0.020	0.040	−0.063	−0.135	0.052	0.266	0.005	−0.022	−0.252	0.253	0.139	0.290	−0.131	0.251	−0.124	−0.239	0.123	0.351
		−0.088	−0.200	−0.034	0.040	0.019	0.025	−0.011	0.022	−0.042	−0.075	0.037	0.146	0.005	−0.009	+0.109	−0.116	−0.062	−0.118	+0.056	−0.104	+0.063	+0.114	−0.064	−0.160
116	2.14	0.281	0.673	0.059	−0.049	−0.035	−0.035	0.017	−0.033	0.065	0.138	−0.052	−0.281	−0.004	0.022	0.271	−0.266	−0.144	−0.297	0.131	−0.245	0.129	0.244	−0.125	0.342
		0.093	0.201	0.025	−0.029	−0.014	−0.020	0.009	−0.017	0.043	0.075	−0.036	−0.151	−0.004	0.009	−0.112	+0.118	+0.063	+0.118	−0.055	+0.101	−0.064	−0.115	+0.064	−0.156
118	1.98	−0.268	−0.670	−0.068	0.055	0.040	0.042	−0.021	0.039	−0.062	−0.124	0.053	0.288	0.005	−0.028	−0.291	0.285	0.152	0.296	−0.132	0.242	−0.138	−0.254	0.127	0.340
		−0.094	−0.211	−0.031	0.034	0.017	0.024	−0.011	0.021	−0.038	−0.089	0.037	0.157	0.005	−0.013	+0.124	−0.129	−0.069	−0.123	+0.058	−0.106	+0.069	+0.123	−0.067	−0.163
120	2.01	0.264	0.670	0.073	−0.056	−0.043	−0.046	0.024	−0.043	0.056	0.107	−0.054	−0.288	−0.005	0.034	0.304	−0.294	−0.156	−0.287	0.129	−0.231	0.139	0.250	−0.126	−0.325
		0.089	0.204	0.033	−0.035	−0.018	−0.026	0.012	−0.023	0.032	0.058	−0.036	−0.152	−0.005	0.015	−0.125	+0.128	+0.070	+0.118	−0.056	+0.101	−0.068	−0.121	+0.065	+0.157
122	2.14	−0.266	−0.700	−0.078	0.053	0.046	0.049	−0.029	0.046	−0.061	−0.111	0.052	0.252	0.004	−0.040	−0.289	0.280	0.150	0.262	−0.118	0.214	−0.132	−0.240	0.117	0.283
		−0.071	−0.168	−0.031	0.031	0.017	0.025	−0.012	0.022	−0.031	−0.057	0.029	0.118	0.005	−0.015	+0.111	−0.113	−0.063	−0.102	+0.049	−0.089	+0.060	+0.109	−0.057	−0.132
124	2.49	−0.289	−0.752	−0.080	0.048	0.047	0.047	−0.031	0.045	−0.059	−0.097	0.048	0.197	0.002	−0.043	−0.255	0.244	0.130	0.222	−0.101	0.180	−0.114	−0.204	0.098	0.221
		−0.042	−0.103	−0.024	0.024	0.013	0.019	−0.009	0.017	−0.023	−0.043	0.018	0.067	0.003	−0.012	+0.083	−0.082	−0.047	−0.074	+0.035	−0.064	+0.044	+0.080	−0.041	−0.092

proton f 7/2 shell, which induces a decrease in the energy of the p 3/2 quasi-particle. The lowest 0^+ core state is found at about 12 MeV.

3.2.1.2 $Z=28$ isotopes. — The lowest 0^+ state is almost purely an open-shell state, with a very weak amount of core components. This state is fairly mixed, with a dominant neutron $(f\,5/2)^2$ two-quasi-particle configuration, and also about 25 % of $(p\,3/2)^2$ admixture. As mass increases, a $(p\,1/2)^2$ admixture develops in this state (30 % in ^{64}Ni). The state is sufficiently collective to keep its excitation energy roughly constant while the quasi-particle energies change as neutron number increases. The lowest core state, almost pure neutron $(f\,7/2)^2$ two-quasi-particle state, is found at about 5 MeV.

3.2.1.3 $N=50$ isotones. — The 0^+ state is again an almost pure open-shell state, with almost vanishing core components. For ^{86}Kr it is almost purely a proton $(f\,5/2)^2$ two-quasi-particle configuration. It becomes fairly mixed for ^{88}Sr; then for ^{90}Zr it is an equal mixture of $(g\,9/2)^2$ and $(p\,1/2)^2$. For ^{92}Mo it is dominantly of a $(p\,1/2)^2$ configuration (60 %). The energy oscillates as a function of mass, as shown by figure 1.

The lowest core state, an almost pure proton $(d\,5/2)^2$ two-quasi-particle configuration, is found at about 7 to 9 MeV.

3.2.1.4 Tin isotopes. — The lowest 0^+ state contains about 70 % of $(s\,1/2)^2$ neutron two-quasi-particle configuration, about 20 % $(h\,11/2)^2$ configuration, a few open-shell components and negligible core components. The amplitudes of configuration mixing are remarkably stable as mass increases from 114 to 124. This moderate mixing may explain the smooth trend with mass number of the energy, as seen in figure 1.

3.2.1.5 Lead isotopes. — The lowest 0^+ state has again negligible core components. It is a fairly mixed state with dominant $(p\,3/2)^2$ neutron two-quasi-particle component for ^{198}Pb, ^{200}Pb, ^{202}Pb, and then with dominant $(p\,1/2)^2$ component for ^{204}Pb and ^{206}Pb. Configuration mixing varies smoothly as mass increases, and the excitation energy remains fairly constant.

3.2.2 2^+ *States.* — We show in figure 2 the energies and electromagnetic transition rates of the calculated lowest two 2^+ levels, together with the energies of two open shell and one core levels contributing to these states. We have displayed the second 2^+ for an appraisal of its frequent two-phonon interpretation. When these lowest two 2^+ states are dominated by open shell contributions, there may be another calculated, low-lying state which is mainly built on core contributions. Such a state is physically interesting and will be discussed in most cases below. The wave functions of the lowest state are given in table VI except for lead because of the large size of its eigenvectors.

3.2.2.1 $N=28$ isotones. — For all three isotones, the excitation energy of the lowest 2^+ state lies close to 1.5 MeV. The magnitudes of the electromagnetic, $T=0$ and $T=1$ transition rates are of the order of 2×10^2, 10^2 and 10^1 respectively for these isotones. This state is a typical two-quasi-particle state, corresponding to an open shell level at about 1.8 MeV excitation energy, with a dominant $(f\,7/2)^2$ component.

The calculated second lowest 2^+ state lies at 3.8 MeV for ^{50}Ti and goes down to 3.1 MeV for ^{54}Fe. It consists mainly of a core contribution made up of the $p\,3/2\,(f\,7/2)^{-1}$ neutron configuration. This core state lies around 3.9 MeV for all three nuclei, and contains significant admixtures of the lowest outside level mentioned above and of a second outside level, dominated by an (f 7/2-p 3/2) configuration, which comes down from 4.7 MeV for ^{50}Ti to 4 MeV for ^{54}Fe. The electromagnetic transition rates associated to the second 2^+ state are about one order of magnitude smaller than those of the first state while the $T=0$ and $T=1$ $B(E2)$ have about the same order of magnitude.

3.2.2.2 Nickel isotones. — The lowest 2^+ state lies around 1.1 MeV and derives mainly from an open shell level around 1.2 MeV which is collective enough to prevent the identification of any dominant configuration. The magnitudes of the electromagnetic, $T=0$ and $T=1$ transition rates are of the order of 90, 3×10^2 and 50, respectively. From a closer examination of our numbers we observe that the electromagnetic and $T=0$ rates have been significantly enhanced by a small admixture of a core level dominated by a proton $p\,3/2\,(f\,7/2)^{-1}$ configuration lying at about 3.4 MeV. Within a good approximation the second 2^+ state lies at twice the excitation energy of the first one. It appears to correspond to a second outside (and weakly collective for ^{58}Ni and ^{60}Ni) level at about 2.5 MeV. The transition rates have no clear relation to the corresponding rate of the first 2^+ state. The only systematic feature is a fast decrease as the mass increases. The reason for this seems to be that the core level at about 3.4 MeV actually moves from 3.1 MeV to 3.8 MeV as mass increases, and contributes less and less to the second 2^+. Such an effect is not expected for the lowest 2^+, because of its high collectivity which makes first order perturbation theory invalid.

We finally mention that after getting mixed in the lowest states, the lowest core state loses a large amount of its strength, while a second core state, at about 4.6 MeV retains all its strength, because it mixes significantly with the open shell levels.

3.2.2.3 N=50 isotones. — The energy of the lowest 2^+ state varies strongly with A (1.4 MeV for ^{86}Kr compared to 2.1 MeV in ^{90}Zr). We observe that this level is not collective and corresponds to an open

shell contribution, at least 70 % of which is made out of a single pure two-quasi-particle configuration. This dominant configuration changes with the filling of the proton shell. A small admixture of a core state (almost purely a proton d 5/2 $(g\ 9/2)^{-1}$ configuration) lying at about 4 MeV, reduces the $T = 1$ transition and increases the $T = 0$ one by a factor of two approximately. The magnitudes of the electromagnetic, $T = 0$ and $T = 1$ transition rates are of the order 3×10^2, 10^2 and 30, respectively. A maximum for the excitation energy and a minimum for all three transition rates are observed at ^{90}Zr.

The second 2^+ state is also rather a pure two-quasi-particle state and its excitation energy varies somewhat as a function of the nuclear mass. It is a fairly pure open shell level, with a small admixture of a core state at about 4 MeV. The $B(E2)$ are approximately one order of magnitude smaller than those of the lowest 2^+, except for ^{90}Zr.

All these purity features are due to the influence of the proton shell closure at $Z = 40$.

3.2.2.4 Tin isotopes. — The trends are similar to those observed in the region of Ni isotopes. Both of the lowest 2^+ states are dominated by open shell collective levels. The two-quasi-particle configurations which contribute mainly to these levels are the neutron $(h\ 11/2)^2$ and (d 3/2 - s 1/2). The lowest core state, almost purely a d 5/2 $(g\ 9/2)^{-1}$ proton configuration, goes up in excitation energy from 4.4 MeV in ^{116}Sn to 4.7 MeV in ^{124}Sn, while both open-shell levels decrease by about 0.2 MeV. The admixture of this core state in the lowest 2^+ is roughly constant while the admixture in the second 2^+ diminishes as the mass increases. As in the case of Ni, this should explain the decrease of the transition rates associated to the second 2^+. For the lowest 2^+ the $B(E2)$ are remarkably constant; the order of magnitudes are 10^2, 6×10^2 and 2×10^2 for the electromagnetic, $T = 0$ and $T = 1$ cases respectively.

3.2.2.5 Lead isotopes. — A collective 2^+ state is found at about 1 MeV, made of a large admixture of open shell, two-quasi-particle configurations. The mixing changes strongly as mass increases, but we notice that the $(f\ 5/2)^2$ configuration always remains one of the largest components. Electromagnetic $B(E2)$, of order 10, are weak, while $T = 0$ and $T = 1$ $B(E2)$ separately are rather strong (about 500). The reason for the weakness of the electromagnetic transition is the small amount of core state, made of a single h 9/2 $(h\ 11/2)^{-1}$ proton configuration lying at about 6 MeV.

A second 2^+ state, less mixed than the first one, is found at about 1.3 MeV. It is also mainly an open shell level, with almost no proton core state admixture. All transition rates are small, although near the doubly magic shell there is an increase in the $T = 0$ and $T = 1$ $B(E2)$.

Besides the proton core state at about 6 MeV, there is a neutron core state at about 5.4 MeV which is mainly a pure (i 11/2 - i 13/2) two-quasi-particle configurations. However, for both core states, transition rates are small.

3.2.3 3^- *States.* — Except for the non normal parity subshell contributions, negative parity levels are made of particle-hole configurations. Thus 3^- states are best suited as indicators of core excitations. In this section we discuss systematically the lowest two 3^- states which are shown in figure 3. The wave functions of the lowest 3^- states are given in table VII, except again for the lengthy lead isotope case.

3.2.3.1 $N=28$ isotones. — The proton open shell could yield 3^- states through f 7/2 - g 9/2 and f 3/2 - g 9/2 two-quasi-particle configurations at low excitation energies. However such states are not found.

Very pure core states appear at about 5 MeV and 7 MeV. The lowest one is very collective, the second one is dominated by a proton p 3/2 $(d\ 3/2)^{-1}$ configuration. For the lowest 3^- state, the magnitudes of the electromagnetic, $T = 0$ and $T = 1$ $B(E3)$ are of order 10^4, 10^4 and 2×10^2, respectively. For the second state, they are of order 8×10^2, 4×10^2 and 5×10^2, respectively.

3.2.3.2 Nickel isotopes. — The lowest 3^- state remains at about 4.2 MeV excitation energy. It is built with a mixture of an open-shell level, almost purely a p 3/2 - g 9/2 neutron two-quasi-particle configuration at about 5.1 MeV, and of a strongly mixed core state at about 5.1 MeV also. The order of magnitudes of the $B(E3)$'s are 8×10^3, 10^4 and 6×10^2, remarkably constant for all the isotopes. This constancy results of course of the core nature of this lowest octupole state.

The second 3^- state starts out as a mixture of the core state and the open-shell configurations which make up the lowest 3^- state, just discussed above. However, as mass increases, a new f 5/2 - g 9/2 two-quasi-particle component, lying at about 6 MeV, builds up and the core state component diminishes. Thus for ^{64}Ni this second 3^- state has become a dominantly open-shell state. The core strength which was shared between the lowest and the second 2^+ states in ^{58}Ni is now shared between the lowest and a third 3^- state, lying at about 6.3 MeV. This explains the sharp drop of the $B(E3)$ strengths of the second state when mass increases.

3.2.3.3 $N=50$ isotones. — The two lowest 3^- states are mainly mixtures of an open-shell state, almost purely made of a p 3/2 - g 9/2 proton two-quasi-particle configuration, and of a core state which is mixed but contains a dominant neutron d 5/2 $(p\ 1/2)^{-1}$ component. Actually, the second 3^- state contains more core components than the first one does, and it also shows a significant amount of a g 9/2 - f 5/2 neutron two-quasi-particle configuration.

For the lowest 3^- state the energies decrease

monotonically as mass increases, which is well correlated with an increase of the transition rates except for the $T = 1$ $B(E3)$ which oscillates. The order of magnitudes of the $B(E3)$'s are 4×10^4, 4×10^4 and 3×10^3. We observe that the electromagnetic and $T = 0$ transition rates have been increased by a factor of about 3 and 10, respectively, from their values yielded by mixing only the open-shell configurations to their values after admixture of the neutron core configurations. On the contrary the $T = 1$ $B(E3)$ is decreased by this admixture by an order of magnitude.

3.2.3.4 Sn isotopes. — In this region, levels of spin and parity 3^- coming from the mixing of open-shell configurations are low enough to compete with the core states. We find a 3^- level at about 2.2 MeV, which is a mixture of an open-shell state, almost purely a d 5/2 - h 11/2 neutron, two-quasi-particle configuration (the energy of which before mixing with the core is about 3.6 MeV) and of a very collective core state also at about 3.6 MeV. The electromagnetic and $T = 0$ $B(E3)$ are of order 10^5 and almost constant for all isotopes. The electromagnetic rate is little changed from that of the core state alone, but the $T = 0$ $B(E3)$ has been enhanced by a factor of about two by the mixing of the open-shell configurations with the core state. On the other hand the $T = 1$ $B(E3)$ has been completely depleted by this mixing and varies from a few units for ^{114}Sn to a few hundred for ^{124}Sn.

The second 3^- state which lies at about 3.7 MeV is made almost purely of a g 7/2 - h 11/2 neutron two-quasi-particle configuration, with a very weak admixture of the core state at about 3.6 MeV mentioned above. Transition rates are fairly weak. The electromagnetic $B(E3)$ increases when mass increases, as shown in figure 3. The $T = 0$ $B(E3)$ decreases from about 10^2 for ^{114}Sn to less than 3 for ^{124}Sn and the $T = 1$ rate increases from about 10^2 to 2×10^2, which means that this second 3^- state would be anyhow hardly detectable and that one should rather look for core states at higher energies. We find some octupole strength at about 5 MeV, but it is about 100 times smaller than the strength of the lowest 3^- state.

3.2.3.5 Pb isotopes. — We observe in Pb isotopes the striking feature of level crossing between open-shell and core states. This occurs at ^{200}Pb, after which the lowest 3^- state changes from a dominant open shell two-quasi-particle state to a core excitation.

The lowest open-shell state, which is almost made of only a i 13/2 - h 9/2 neutron two-quasi-particle configuration for all nuclei except ^{206}Pb, plays the role of the dominant component for the lowest 3^- state in ^{198}Pb. It contributes to the lowest two 3^- states for ^{200}Pb, then makes up most of the second lowest state for ^{202}Pb and ^{204}Pb. It becomes high lying for ^{206}Pb.

The second open-shell state is almost purely a i 13/2-f 7/2 neutron two-quasi-particle configuration. For ^{198}Pb and ^{200}Pb it contributes to the lowest three 3^- states, then becomes high lying for the other isotopes. In ^{202}Pb the lowest 3^- state is collective enough to retain a small component on this open shell state.

The lowest core state is very collective. For ^{198}Pb and ^{200}Pb it contributes to the lowest three 3^- states and is dominant in the third state for ^{198}Pb. For ^{202}Pb, ^{204}Pb and ^{206}Pb it is dominant in the lowest 3^- state. Thus, except for ^{200}Pb which shows strong mixtures for all low lying states, and for ^{198}Pb, where the lowest two states are of an open-shell nature, it appears that the lowest 3^- state in Pb isotopes is primarily a core excitation.

The electromagnetic, $T = 0$ and $T = 1$ $B(E3)$'s for the lowest state are of order of magnitude 4×10^5, 5×10^5 and 4×10^4, respectively for nuclei where the core state has become the lowest one, namely for ^{202}Pb to ^{206}Pb. A smooth increase of about 20 % is observed in this case as mass increases. For ^{198}Pb and ^{200}Pb, the rates are of course very sensitive to the amount of core components. The rates are about 10 times smaller for ^{198}Pb and 3 times smaller for ^{200}Pb.

Some remaining strength is found in the second 3^- state for ^{198}Pb and for ^{200}Pb. For all other isotopes, the higher octupole states are much weaker than the lowest one.

3.2.4 4^+ *States.* — The lowest calculated 4^+ state, figure 4, is essentially made of open-shell configurations. It may contain, however, small but significant amounts of core components, coming from a core state which is often found at about 2 MeV higher, as discussed below.

3.2.4.1 $N=28$ isotones. — The state is almost purely a $(f\ 7/2)^2$ proton, two-quasi-particle configuration, at about 2 MeV. It receives a small admixture from core states, almost purely made of neutron p 3/2 $(f\ 7/2)^{-1}$ and p 1/2 $(f\ 7/2)^{-1}$ configurations, lying at about 4 and 5 MeV, respectively.

The magnitudes of the electromagnetic, $T = 0$ and $T = 1$ $B(E4)$ are of order 10^5, 7×10^4 and 4×10^3, respectively. They are fairly constant for all three isotones. The second 4^+ state has an electromagnetic rate about ten times smaller than the one of the lowest 4^+ state a $T = 0$ rate about equal, and a $T = 1$ rate a few times larger.

3.2.4.2 *Nickel isotopes.* — The lowest state lies at about 2.0 MeV and contains about 70 % of a (p 3/2 - f 5/2) neutron two-quasi-particle configuration. The remainder comes from a second open-shell state, made of an almost pure $(f\ 5/2)^2$ configuration at about 3.1 MeV, and from a mixed core state lying at about 4 MeV, the dominant components of which are proton and neutron p 3/2 $(f\ 7/2)^{-1}$ particle-hole configurations.

The magnitudes of the electromagnetic, $T = 0$ and $T = 1$ $B(E4)$ are of order 5×10^4, 10^5 and 3×10^4, respectively. They are fairly constant for all four isotopes. The higher excited 4^+ states have much smaller $T = 1$ $B(E4)$. The electromagnetic rates of the core state at about 4 MeV are of the same order of magnitude as the rates for the lowest state, and the $T = 0$ rates are a few times smaller.

3.2.4.3 $N = 50$ isotones. — For ^{86}Kr and ^{88}Sr the lowest 4^+ is almost purely a p 3/2 - f 5/2 proton, two-quasi-particle configuration. For ^{90}Zr and ^{92}Mo, it is almost purely a $(g\ 9/2)^2$ configuration. The open-shell states are very pure two-quasi-particle configurations and their relative positions change in a way very sensitive to the single-quasi-particle energies. The lowest core state is more stable, lying between 4.2 and 4.6 MeV. It contains almost 90 % of a d 5/2 $(g\ 9/2)^{-1}$ neutron configuration. The admixture of core levels into the lowest 4^+ state is anyhow negligible for all four isotones. The electromagnetic, $T = 0$ and $T = 1$ $B(E4)$ for the lowest 4^+ are of order 10^5, 7×10^4 and 2×10^4, respectively, with a minimum for ^{88}Sr. Electromagnetic rates for higher excited 4^+ states are much smaller, while the core state at about 4.4 MeV (average) shows $T = 0$ and $T = 1$ rates of order 2×10^6. The other states have weaker $T = 0$ and $T = 1$ rates.

3.2.4.4 Sn isotopes. — Two states are found at about 2.3 and 3.1 MeV, which are mainly a mixture of open-shell configurations, with often a slight dominance of the neutron g 7/2 - d 3/2 two-quasi-particle configuration. However configuration mixing changes very much from one isotope to another. These lower states contain small admixtures of two core states, lying at about 4.6 and 5.3 MeV, which are moderately mixed states. The lowest core state contains about 70 % of the proton g 7/2 $(g\ 9/2)^{-1}$ configuration and the second core state contains about 70 % of the proton d 5/2 $(g\ 9/2)^{-1}$ particle-hole configuration.

The magnitudes of the $B(E4)$ for the lowest 4^+ state are about 4×10^5, 10^6 and 2×10^5 and fairly constant for all isotopes. The $B(E4)$ of the second state are at least a few times smaller. In contrast, the core states which come as third and fourth 4^+ states show high transition rates, for they lose little strength through admixture in the lowest state.

The $B(E4)$ for the lowest core states are about 10^6, 2×10^5 and 4×10^5 and the second core state is about half as strong.

4. **Conclusions.** — This analysis of the S.C.S. even nuclei within the two-quasi-particle and particle-hole space including the two major shells nearest to the Fermi level has been successful in two respects.

i) The energies of the lowest *vibrational* states are well obtained for *all* studied nuclei, with no parameter fiddling. The quasi-particle energies are the experimental levels of the odd-even nuclei, the u's and v's and the even $T = 1$ force are uniquely given by the I.G.E. procedure and the ratio of the even $T = 0$ to the even $T = 1$ force components kept to the fixed value of 1.25 throughout the table.

ii) The transition properties of all octupole states are properly obtained. On the other hand, in view of these agreements, it may be surprising to find vast differences between computed and experimental $B(E2)$ and $B(E4)$. In these cases the simple particle-hole excitations of the core play actually a negligible role, and the results indicate the need for more complicated processes leading to large even parity core proton contributions in the low lying spectrum. Two and four particle-hole components have been shown to be negligibly small in the wave function of the first 2^+ state of ^{58}Ni ([1]). Of course particle-hole excitations across two major shell ($\Delta n = 2$), neglected here, may play a certain role through their large quadrupole matrix elements.

Acknowledgments. — The authors whish to thank Jean Picard for his participation in the computing of the $N = 50$ case. They are very grateful to Mrs. Nicole Tichit for her extremely precious computational help without which this work could not have been completed.

We shall be happy to send on request the wave functions for the lead isotopes too lengthy to be presented here.

APPENDIX

The matrix elements of the effective force V between two quasi-particle states entering eq. (5) are given by

$$\langle (ab)\, J \mid V \mid (cd)\, J \rangle = [(1 + \delta_{ab})(1 + \delta_{cd})]^{-1/2} \{ (u_a u_b u_c u_d + v_a v_b v_c v_d)\, G(abcdJ) - $$
$$- (u_a v_b u_c v_d + v_a u_b v_c u_d)\, F(abcdJ) + (-)^{j_c + j_d + J} (u_a v_b u_d v_c + v_a u_b v_d u_c)\, F(abdcJ) \}$$

and

$$\langle (ab)\, J \mid V \mid (\widetilde{cd})\, J \rangle = - [(1 + \delta_{ab})(1 + \delta_{cd})]^{-1/2} \{ (u_a u_b v_c v_d + v_a v_b u_c u_d)\, G(abcdJ) +$$
$$+ (u_a v_b u_d v_c + v_a u_b v_d u_c)\, F(abcdJ) - (-)^{j_c + j_d + J} (u_a v_b u_c v_d + v_a u_b v_c u_d)\, F(abdcJ) \}$$

([1]) Jaffrin, A., Private communication.

where $G(abcdJ)$ is the usual particle-particle matrix element for the effective force V between the 2-particle configurations $|\,(ab)\,J\,\rangle$ and $|\,(cd)\,J\,\rangle$

$$|\,(ab)\,JM\,\rangle = \sum_{m_a m_b} (j_a j_b\, m_a\, m_b \,|\, JM)\, \eta_a^+\, \eta_b^+\, |\,\rangle\,,$$

while $F(abcdJ)$ is the *particle-hole* matrix element given by the transformation,

$$F(abcdJ) = -\sum_{J'} (-)^{j_a + j_b + j_c + j_d} \times$$

$$\times\, (2J' + 1) \begin{Bmatrix} d & a & J' \\ b & c & J \end{Bmatrix} G(dabcJ')\,.$$

The amplitudes X and Y given in the tables correspond to the choice of phases of eq. (1) for the coupling of 2-quasi-particle states, of eq. (2) for the quasi-particle transformation, and using the single particle coupling $\mathbf{l} + \mathbf{s}$ in that order, radial orbitals positive for large r together with an angular part defined as :

$$\mathcal{Y}_m^l(\hat{r}) = i^l\, Y_m^l(\hat{r})\,.$$

This last definition ensures that all v's are chosen real and positive.

The matrix elements of the one body operator entering eq. (6) with these phases are then given by

$$\langle\, \alpha \,|\, \theta^J \,|\, \beta \,\rangle = \frac{1}{\sqrt{1 + \delta_{\alpha\beta}}} (u_\alpha v_\beta + v_\alpha u_\beta) \langle\, \alpha \,||\, \theta^J \,||\, \beta \,\rangle$$

and

$$\langle\, \alpha \,||\, \theta^J \,||\, \beta \,\rangle = (-)^{j_\alpha - 1/2 + (J + l_\alpha - l_\beta)/2} \times$$

$$\times \sqrt{(2J + 1)\,(2j_\alpha + 1)\,(2j_\beta + 1)} \begin{pmatrix} j_\beta & j_\alpha & J \\ 1/2 & 1/2 & 0 \end{pmatrix}$$

$$\times \int r^2\, \mathrm{d}r \varphi_{n_\alpha l_\alpha}(r)\, r^J\, \varphi_{n_\beta l_\beta}(r)\,.$$

As a check one may verify that all the contributions to the transition rates, eq. (6), add up in the case of the lowest vibrational state. This property, true of a separable force [8], is still valid for a finite range gaussian force because of the dominance of the direct term in the particle hole matrix element and the near separability of the gaussian force.

References

[1] For review, see BARANGER, E., *Advances in Nuclear Physics* **4** (Plenum Press, New York) 1971, p. 361 where an extensive reference is given.

[2] GILLET, V., GIRAUD, B. and RHO, M., *Nucl. Phys.* **A 103** (1967) 257.

[3] GILLET, V., GIRAUD, B., PICARD, J. and RHO, M., *Phys. Lett.* **27B** (1968) 483.

[4] GILLET, V., GIRAUD, B. and RHO, M., *Phys. Rev.* **178** (1969) 1695.

[5] BARANGER, M., *Phys. Rev.* **120** (1960) 957.
ARVIEU, R., *Annls. de Phys.* **8** (1963) 407.

[6] MOTTELSON, B., *Proc. of the International School Enrico Fermi*, Session XL (Academic Press Inc., New York, 1960) 45.

[7] BERNSTEIN, A., *Adv. Nucl. Phys.* **3** (Plenum Press New York) (1970) 325.

[8] BROWN, G. E. and BOLSTERLI, M., *Phys. Rev. Lett.* **3** (1959) 472.

[9] THOULESS, D. J., *Nucl. Phys.* **22** (1961) 78.

[10] PHAN XUAN HO, BELLICARD, J. B., LECONTE, Ph. and SICK, I., Proceedings of the International Conference on Nuclear Structure Using Electron Scattering and Photonuclear Reactions, Sendaï (1972).

[11] SCHAEFFER, R., *Nucl. Phys.* **A 135** (1969) 231.

[12] BRISSAUD, I., TATISCHEFF, B., BIMBOT, L., COMPARAT, V., WILLIS, A. and BRUSSEL, M. K., *Phys. Rev.* **C 6** (1972) 595.